OPTICAL COHERENCE TOMOGRAPHY ANGIOGRAPHY FOR CHOROIDAL AND VITREORETINAL DISORDERS - PART 2

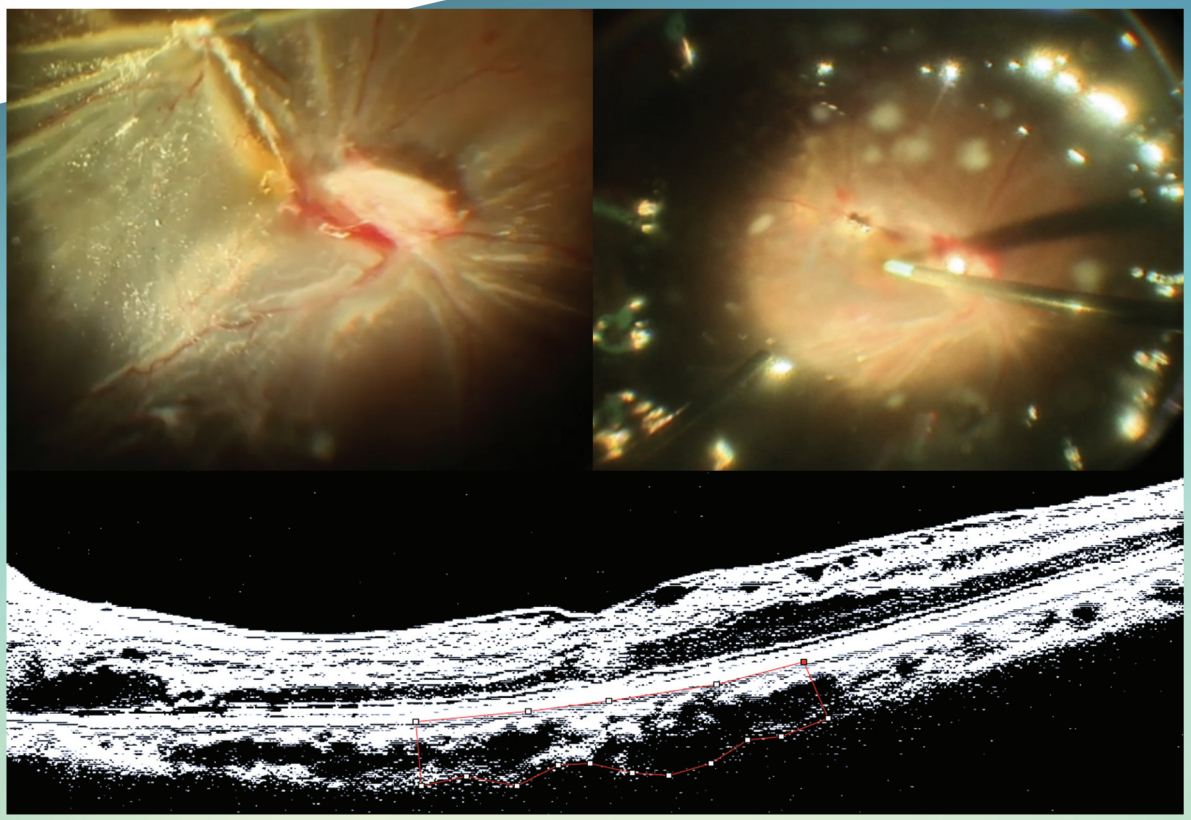

Editors:
Miguel A. Quiroz-Reyes
Virgilio Lima-Gomez

Bentham Books

Optical Coherence Tomography Angiography for Choroidal and Vitreoretinal Disorders Part 2

Edited By

Miguel A. Quiroz-Reyes
Oftalmologia Integral ABC, Retina Department
Medical and Surgical Assistance Institution (Nonprofit Organization)
Affiliated with the Postgraduate Studies Division
National Autonomous University of Mexico
Mexico City, Mexico

&

Virgilio Lima-Gomez
Ophthalmology Service, Hospital Juarez de Mexico
Public Assistance Institution (Nonprofit Organization)
Mexico City, Mexico

Optical Coherence Tomography Angiography for Choroidal and Vitreoretinal Disorders – Part 2

Editors: Miguel A. Quiroz-Reyes & Virgilio Lima-Gomez

ISBN (Online): 978-981-5196-65-8

ISBN (Print): 978-981-5196-66-5

ISBN (Paperback): 978-981-5196-67-2

First published in 2023.

need for a court order if at any point you breach any terms of this License Agreement. In no event will any delay or failure by Bentham Science Publishers in enforcing your compliance with this License Agreement constitute a waiver of any of its rights.

3. You acknowledge that you have read this License Agreement, and agree to be bound by its terms and conditions. To the extent that any other terms and conditions presented on any website of Bentham Science Publishers conflict with, or are inconsistent with, the terms and conditions set out in this License Agreement, you acknowledge that the terms and conditions set out in this License Agreement shall prevail.

Bentham Science Publishers Pte. Ltd.
80 Robinson Road #02-00
Singapore 068898
Singapore
Email: subscriptions@benthamscience.net

CONTENTS

FOREWORD

There is no doubt that serendipity plays an important role in many scientific developments. One very clear example is the evolution of Ophthalmic Coherence Tomography (OCT) in Ophthalmology.

In the early 1970s, Michel Duguay at the AT & T Bell Laboratories published "Light photographed in flight", where he proposed that echoes of light could be used to examine biological tissue. In the mid-1970s, Erich Ippen, of Massachusetts Institute of Technology (MIT), further developed femtosecond optics. Both discoveries built the foundation of the concept called optical reflectivity, with the idea that light interference could be used to obtain a non-invasive "biopsy" of translucid tissues. In the late 1980s, corneal refractive surgery was at its summit. It required an accurate measurement of corneal thickness. James Fujimoto of MIT collaborated with Ophthalmologists Joel Schuman, David Huang and Carmen Puliafito to refine this measurement, using low-coherence interferometry with only partial success. Nevertheless, in a poorly focused image of the cornea, Huang noticed what appeared to be an optical section of the retina in the background. Instead of dismissing this poorly defined image as useless, Huang continued experimenting until he was able to obtain an optical transverse image of the retina. Thus, retinal and choroidal OCT was born. Today OCT constitutes the most important ancillary test and standard of care in Ophthalmic practice, not only in vitreoretinal pathology, but also in glaucoma and problems of the anterior segment.

More recently, swept-source OCT, which can produce 500,000 scans per second and OCT angiography, employing motion contrast imaging, allow us to image retinal capillaries and the smallest neo-vessels in the retinal tissues. Also, enhanced penetration has allowed to provide detailed visualization of the choroid. New technologies are in constant development, such as visible light OCT (visOCT) and adaptive optics (AO-OCT) will allow further details and deeper penetration.

In this particular section of the book, after a review of general principles and advances of OCT and OCTa use in vitreoretinal disorders, all the contributors and coauthors engage in describing to us the normal and pathological parameters of macular and choroidal perfusion patterns, followed by a description and findings in several vitreoretinal and choroidal pathological disorders.

There is no doubt that all the new and described findings in this book will widen our knowledge and be of benefit to our ailing patients.

Alexander Dalma M.D.
Dr. Dalma y Asociados, UNAM
Ciudad de Mexico, Mexico

PREFACE

Optical coherence tomography angiography is one of the most important recent innovations in ophthalmology. The book you have in your hands represents the collaborative efforts of a select team of subject matter experts. This book aims to be a practical, patient-centered guide complemented with a clinical approach and demonstrative clinical cases to assist ophthalmologists and ophthalmology trainees in the evaluation of newly developed perfusion concepts and the diagnosis and management of patients presenting with a wide spectrum of diseases of the retina and choroid, as well as the role of perfusion parameters in the pathogenesis of diverse diseases. As mentioned briefly before, this book describes the journey from basic ophthalmology principles to the most sophisticated current aspects and advances that have resulted in the development of superb technological innovations. We have gone from fundus fluorescein angiography imaging to the evaluation of the perfusional indices of retinochoroidal structures using noninvasive and noncontact imaging techniques that allow a high histopathological correlation of structural tissue characterization with microvascular evaluation on tissue perfusion.

Written by leading international experts in the field, *Optical Coherence Tomography Angiography for Choroidal and Vitreoretinal Disorders* serves as a practical tool for daily work in a retina clinic, helping you through the first steps of perfusion investigation and clinical evaluation, correlation management and treatment decisions for these complex patients. Each chapter details distinct diseases of the retina or choroid, with a focus on signs and perfusion; optical coherent tomography is emphasized, and the chapters are illustrated with many multipaneled images, such that the book may be used as a reference for deciding on diagnostic and treatment options.

This book dissects the basics of angiography by optical coherence tomography and explains the differences in the clinical utility of optical coherence tomography as well as its complementarity. This gives us a broad explanation of the nomenclature and normal perfusional findings in healthy populations.

Several chapters explain macular perfusional findings in different vitreoretinal and choroidal pathologies, including vascular entities commonly seen in daily practice, such as diabetic retinopathy, hemorrhagic and ischemic infarctions of the retina due to vascular disorders, and choroidal pathological neovascularization; most importantly, perfusion parameters are evaluated by quantification and binarization of the different vascular plexuses at the retinal and choroidal level. Additionally, certain tractional entities are evaluated from the point of view of their microstructural findings and perfusional postoperative outcomes, associating them with the final vision.

Some chapters deal with new antivascular endothelial growth factor molecules and new extended-release delivery devices and provide a comparative evaluation of the therapeutic effect on perfusion. In this way, multiple complex pathological disorders of the retina and choroid are more efficiently diagnosed, followed by natural and treated medical or surgical evolution according to the specific cause and consequently, as mentioned before, monitored in response to specific treatments.

We hope that this book, from a multitude of experts, contributes pertinently to academia and achieves the objective of serving as a guide both in the diagnosis and clinical decision-making that those of us who are dedicated to the difficult but beautiful and challenging practice of clinical and surgical retina care perform on a daily basis.

Miguel A. Quiroz-Reyes, MD
Oftalmologia Integral ABC, Retina Department
Medical and Surgical Assistance Institution (Nonprofit Organization)
Affiliated with the Postgraduate Studies Division
National Autonomous University of Mexico
Mexico City, Mexico

&

Virgilio Lima-Gomez, MD
Ophthalmology Service, Hospital Juarez de Mexico
Public Assistance Institution (Nonprofit Organization)
Mexico City, Mexico

List of Contributors

Alejandra Nieto-Jordan	Institute of Ophthalmology, Fundacion Conde de Valenciana, Private Assistance Institution (Nonprofit Organization), Mexico City, Mexico
Aftab Taiyab	Department of Pathology and Molecular Medicine, McMaster University, Hamilton, Canada
Caleb Llacctarimay, MD	Hospital Nacional Sergio E. Bernales, Lima, Peru
Erick A. Quiroz-Gonzalez	Oftalmologia Integral ABC, Retina Department, Medical and Surgical Assistance Institution (Nonprofit Organization), Affiliated with the Postgraduate Studies Division, National Autonomous University of Mexico, Mexico City, Mexico Institute of Ophthalmology, Fundacion Conde de Valenciana, Private Assistance Institution (Nonprofit Organization), Mexico City, Mexico
Felipe Esparza-Correa	Institute of Ophthalmology, Fundacion Conde de Valenciana, Private Assistance Institution (Nonprofit Organization), Mexico City, Mexico
Geraint J. Parfitt	School of Optometry & Vision Sciences, Cardiff University, Cardiff, United Kingdom
Jose A. Roca-Fernandez, MD	Cayetano Heredia University, Lima, Peru Retina Division, Ricardo Palma Clinic, Lima, Peru
Jorge Morales-Navarro	Institute of Ophthalmology, Fundacion Conde de Valenciana, Private Assistance Institution (Nonprofit Organization), Mexico City, Mexico
Jorge E. Aceves-Velazquez	Institute of Ophthalmology, Fundacion Conde de Valenciana, Private Assistance Institution (Nonprofit Organization), Mexico City, Mexico
Juan Pablo Dávila-Gonzalez	Dalma y Asociados SC. Mexico City, Mexico
José Dalma-Weiszhausz	Asociacion para prevenir la Ceguera en Mexico, Mexico City, Mexico
Jennifer H. Kim-Lee	Institute of Ophthalmology, Fundacion Conde de Valenciana, Private Assistance Institution (Nonprofit Organization), Mexico City, Mexico
Miguel A. Quiroz-Reyes, MD	Oftalmologia Integral ABC, Retina Department, Medical and Surgical Assistance Institution (Nonprofit Organization), Affiliated with the Postgraduate Studies Division, National Autonomous University of Mexico, Mexico City, Mexico
Margarita Montano	Oftalmologia Integral ABC, Retina Department, Medical and Surgical Assistance Institution (Nonprofit Organization), Affiliated with the Postgraduate Studies Division, National Autonomous University of Mexico, Mexico City, Mexico
Miguel A. Quiroz-Gonzalez	Oftalmologia Integral ABC, Retina Department, Medical and Surgical Assistance Institution (Nonprofit Organization), Affiliated with the Postgraduate Studies Division, National Autonomous University of Mexico, Mexico City, Mexico
M. Naveed Yasin	Department of Ophthalmology, The University of Auckland, Auckland, New Zealand Department of Pathology and Molecular Medicine, McMaster University, Hamilton, Canada

Nathaly V. Huaman-Mendez, MD	Retina Division, Ricardo Palma Clinic, Lima, Peru
Sanjay Marasini	Department of Ophthalmology, The University of Auckland, Auckland, New Zealand
Virgilio Lima-Gomez, MD	Ophthalmology Service, Hospital Juarez de Mexico, Public Assistance Institution (Nonprofit Organization), Mexico City, Mexico
Zixuan Shao	Division of Chemistry and Chemical Engineering, California Institute of Technology, Pasadena, CA, USA

CHAPTER 1

Sequelae and Macular Perfusion Repercussions in Obstructive Venous Vascular Phenomena of the Retina

Geraint J. Parfitt[1] and **Miguel A. Quiroz-Reyes, MD**[2,*]

[1] *School of Optometry & Vision Sciences, Cardiff University, Cardiff, United Kingdom*

[2] *Oftalmologia Integral ABC, Retina Department, Medical and Surgical Assistance Institution (Nonprofit Organization), Affiliated with the Postgraduate Studies Division, National Autonomous University of Mexico, Mexico City, Mexico*

Abstract: Venous drainage from the retina merges into the central retinal vein and can be obstructed in the branch veins that drain the retinal quadrants, or the central retinal vein itself, which are termed Branch Retinal Vein Occlusion (BRVO) and Central Retinal Vein Occlusion (CRVO), respectively. Obstruction of retinal venous drainage often leads to a sudden or progressive increase in distal venous and capillary pressure with loss of vision and visual field defects. The extent of visual impairment correlates with the location and severity of the venous occlusion and how it impacts perfusion in the retina. Macular edema or retinal ischemia secondary to retinal vein occlusion is responsible for vision loss in retinal vein occlusions, and the advent of anti-VEGF therapeutics has revolutionized the management of vascular disease in the retina.

In this chapter, we review our current understanding of retinal vein occlusions and how OCT-Angiography (OCT-A) is being used clinically in the diagnosis and management of obstructive venous vascular phenomena. The benefits of using OCT-A in the diagnosis and management of CRVO and BRVO over conventional approaches, such as Fundus Fluorescein Angiography (FFA), are discussed. The current limitations of OCT-A and recent advances in the technology are also covered here. Finally, we assess how OCT-A can play a role in the development of new therapeutics to tackle one of the major causes of vision loss worldwide.

* **Corresponding author Miguel A. Quiroz-Reyes, MD:** Oftalmologia Integral ABC, Retina Department, Medical and Surgical Assistance Institution (Nonprofit Organization), Affiliated with the Postgraduate Studies Division, National Autonomous University of Mexico, Mexico City, Mexico; Tel: +525 5217 2732; Fax: +525 55 1664 7180; E-mails: drquiroz@prodigy.net.mx and drquirozreyes7@gmail.com

Miguel A. Quiroz-Reyes and Virgilio Lima-Gomez (Eds.)

Keywords: Binarized, Branch retinal vein occlusion, Central retinal vein occlusion, Deep capillary plexus, Hemiretinal vein occlusion, Optical coherence tomography angiography, Macular edema, Neovascularization, Relative afferent pupillary defect, Retinal ischemia, Retinal vein occlusion, Skeletonization, Superficial capillary plexus.

INTRODUCTION

The retina is a highly metabolic tissue that requires a large volume of arterial blood inflow, and venous drainage, to prevent retinal hypoxia and the subsequent cell viability and vision loss. Arterial blood vessels of the retina supply oxygen to the inner neurons through the superficial capillary plexus (SCP), whereas the avascular region comprised of photoreceptors and retinal pigment epithelium relies on the choriocapillaris and deep capillary plexus (DCP) for providing oxygen by diffusion. Venous drainage of retinal blood vessels converges at the central retinal vein, which passes through the lamina cribrosa of the optic nerve head, and then drains into the superior ophthalmic vein or cavernous sinus. Central retinal vein occlusion (CRVO) and branch retinal vein occlusion (BRVO) are defined as a blockage of the veinous drainage from the eye in either the central vein, or one of the four branch veins that drain each quadrant of the retina, respectively.

Obstructive Venous Vascular Phenomena of the Retina and Optical Coherence Tomography Angiography (OCT-A)

Retinal vein occlusion (RVO) is the second most prevalent vascular pathology in the retina after diabetic retinopathy [1] and is a major contributor to vision loss. Currently, there is an estimated 16 million adults affected by RVO [1], and the prevalence of venous retinal occlusion is approximately 0.7% to 1.6%, according to a previous study conducted in Australia [2]. RVO can be subdivided into central retinal vein occlusion (CRVO); hemi-retinal vein occlusion (HRVO); or branch retinal vein occlusion (BRVO), according to the site of venous obstruction. It is predicted that 2.5 million people are affected by CRVO, while 13.9 million are affected by BRVO [3]. The prevalence and five-year incidence of BRVO are both 0.6%, while CRVO prevalence is found to be lower at 0.1%, with a five-year incidence of 0.2% [4]. The incidence of CRVO in the non-affected eye is 7% within four years [5]. The prognosis of RVO is mainly dependent on the region, extent, duration, and intensity of retinal ischemia as retinal neurons become starved of oxygen [1].

RVO can be diagnosed by a combination of fundus features, including retinal vascular dilation and tortuosity, cotton-wool exudates, flame-shaped retinal hemorrhages, optic disc swelling, and macular edema. Retinal hemorrhages will

be present in all four quadrants of the fundus in CRVO, while they are confined to either the superior or inferior hemisphere of the fundus in HRVO. On the other hand, BRVO is characterized by hemorrhages localized to the area drained by the occluded branch retinal vein [6]. Vision loss is a consequence of macular edema or retinal ischemia secondary to RVO and retinal hypoxia. This chapter outlines how OCT-A is being used to evaluate obstructive venous vascular phenomena of the retina and their sequelae.

Optical Coherence Tomography (OCT) is a non-invasive imaging technique that uses low-coherence interferometry to obtain high-resolution, cross-sectional images of biological tissues *in vivo*, such as the retina. It is particularly valuable for imaging transparent or semi-transparent tissues and plays a crucial role in ophthalmology for diagnosing and monitoring retinal disease. OCT is based on the principles of interferometry and utilizes light waves to measure the time delay and intensity of backscattered or reflected light from tissue structures.

The basic setup of an OCT system consists of a light source, interferometer, sample arm, reference arm, and detector. Typically, a near-infrared light source with a broad bandwidth, such as a superluminescent diode or femtosecond laser, is used. The light is split into two paths: the sample arm, directed towards the tissue being imaged, and the reference arm, directed towards a mirror. The light beams recombine, and interference between the light waves from the sample and reference arms occurs. The interference signal is captured by a high-speed detector, such as a charge-coupled device (CCD) camera. By measuring the intensity of the interference pattern as a function of the reference arm mirror position, information about the depth or distance from the reference mirror to different tissue structures can be obtained. This depth-resolved information is used to construct cross-sectional images of the retina.

Low-coherence interferometry, a fundamental principle underlying OCT, was invented by physicist Endre M. György in 1965. In the early 1990s, David Huang, Carmen Puliafilto, James Fujimoto, and their colleagues developed the first Time-Domain OCT (TD-OCT) system for ophthalmic imaging [7], and commercial TD-OCT systems first became available in 1996. Maciej Wojtkowski's research team introduced Spectral-Domain OCT (SD-OCT), also known as Fourier-Domain OCT, which uses a spectrometer to measure the spectrum of backscattered light and enables faster imaging with higher resolution [8]. One of the key advantages of OCT is its high resolution, which allows for detailed visualization of tissue microstructures. The axial resolution of OCT is determined by the coherence length of the light source, while the lateral resolution is determined by the focusing optics and the beam diameter. With modern OCT

CHAPTER 2

Optical Coherence Tomography Angiography Findings and Evaluation in Regional and Diffuse Retinal Infarction

Jose A. Roca-Fernandez, MD[1,2,*], Nathaly V. Huaman-Mendez, MD[2] and **Caleb Llacctarimay, MD[3]**

[1] *Cayetano Heredia University, Lima, Peru*

[2] *Retina Division, Ricardo Palma Clinic, Lima, Peru*

[3] *Hospital Nacional Sergio E. Bernales, Lima, Peru*

Abstract: Optical Coherence Tomography- Angiography (OCT-A) can separately detect the superficial vascular plexus and the deep vascular plexus. Paracentral acute middle maculopathy (PAMM) is an idiopathic or secondary entity to a local retinal vascular or systemic disease, characterized by capillary vascular occlusions. Some authors recognize it as a variant of acute macular neuroretinopathy (AMN). In general, the most frequent findings in the acute phase are a slight decrease in deep capillary plexus (DCP) perfusion, and hyperreflectivity of the middle layer; in the chronic phase, the findings are DCP hypoperfusion and hyporeflectivity of the middle layer.

Keywords: Retinal infarction, Paracentral acute middle maculopathy, PAMM, Vascular occlusion, Superficial capillary plexus, Deep capillary plexus, OCT-angiography.

INTRODUCTION

Classical histological publications highlight that there are two parallel vascular networks at the level of the internal retina, the superficial vascular plexus and the deep vascular plexus; the superficial vascular plexus consist of 75 microns vessels located between the nerve fiber layer (NFL) and the ganglion cell layer (GCL), it originates directly from arterioles and is the source of origin of the venula; the deep vascular plexus is represented by a dense and complex system of smaller

[*] **Corresponding author Jose A. Roca-Fernandez, MD:** Cayetano Heredia University, Lima, Peru; Retina Division, Ricardo Palma Clinic, Lima, Peru; Tel: +5112246593; Fax: +5112241603; ORCID ID: 0000 0002 9619 9178; E-mail: jaroca62@gmail.com

Miguel A. Quiroz-Reyes and Virgilio Lima-Gomez (Eds.)

vessels (20 microns) into the outer plexiform layer (OPL). Both networks are interconnected through small vessels of vertical course.

Optical Coherence Tomography- Angiography (OCT-A) can separately detect the superficial vascular plexus in the ganglion cell layer and the deep vascular plexus in the outer plexiform layer. These two networks have different aspects, which are not appreciated with standard angiography.

In healthy eyes, the superficial vascular plexus consists of larger vessels that end in the foveal avascular zone (FAZ). Deep vessels show an interconnected network of smaller dense vessels.

OCT-A allows identify four capillary networks/plexuses within the posterior pole. The superficial system is located predominantly within the GCL, known as the superficial capillary plexus (SCP), and to a lesser extent within the NFL, where it is most prominent around the optic nerve and is known as the radial peripapillary plexus. The deep system consists of an intermedia capillary plexus (ICP) within the inner portion of the inner nuclear layer (INL) bordering the inner plexiform layer (IPL) and a deep capillary plexus (DCP) within the outer portion of the inner nuclear layer (INL) bordering the outer plexiform layer (OPL).

Paracentral acute middle maculopathy (PAMM) is an idiopathic or secondary entity to a local retinal vascular or systemic disease, characterized by capillary vascular occlusions. There are reports associating it with different retinal vascular diseases, including diabetic retinopathy, retinal artery occlusion, central retinal vein occlusion, sickle cell retinopathy, Purtscher's retinopathy, hypertensive retinopathy, post upper respiratory tract infection, Covid-19 infection, among others, supporting ischemic pathogenesis.

Some authors recognize it as a variant of acute macular neuroretinopathy (AMN). Sarraf *et al.* have defined two forms of AMN, type 1 or PAMM, characterized by SD-OCT findings at the level of the inner nuclear layer (INL), and AMN type 2, which is associated with outermost layers of the retina abnormalities in the macular area. The mean age of patients with PAMM is 59 years and is described predominantly in men, while patients with traditional AMN lesions had a mean age of 33 years and tended to be women [1]. However, other authors consider that they are two distinct disorders with some overlapping characteristics.

In the fundus, compared to cotton-wool spots, the retinal whitening associated with PAMM lesions is markedly different, with a duller, less opaque grayish-white color, deeper in the retina, and without following the distribution of the nerve fiber layer.

OCT-A is recorded in conjunction with OCT-B scans, from the same location, allowing simultaneous visualization of structure and blood flow. Optical coherence tomography allows to evidence hyperreflective lesions in the form of an INL band, characteristic of PAMM in the acute phase, that eventually resolve in weeks, giving INL thinning, indicative of old PAMM lesions or old INL infarction. OCT-A during this chronic phase usually demonstrates loss of flow within the DCP, which can be self-limiting due to the mechanism of vascular reperfusion. [2].

With the advent of OCT-A, PAMM has emerged as a vascular pathology, however, it is important to complement the study of this "new" pathology with multimodal imaging and Spectral Domain OCT (SD-OCT).

While it is true that OCT-A studies have shown that both PAMM and AMN lesions are associated with capillary vascular occlusions, the affected primary capillary plexus remains controversial, and possibilities include superficial (SCP), intermediate (ICP), and deep capillary plexuses (DCP), as well as choriocapillaris.

Chu S and col. found that PAMM is associated with reduced blood flow at the level of SCP and DCP, ICP alone, or ICP and DCP. While AMN has been associated with occlusion of the deep capillary plexus (DCP) or the choriocapillaris [2].

PAMM lesions can be focal or diffuse; the focal lesions are related to perfusion preservation of the deep capillary plexus; the diffuse lesions, are seen in central retinal artery occlusion (CRAO), where there is a severe DCP lack of perfusion in the acute and chronic cases [3, 6]. The mechanism of ischemia and reperfusion explains the immediate microcirculation restoration observed in some of the focal lesions, however, in obstruction of large vessels, capillary reperfusion may not occur [4].

In general, the most frequent findings in the acute phase are a slight decrease in DCP perfusion, and focal or multifocal or diffuse hyperreflectivity of the middle layer; in the chronic phase, the findings are DCP hypoperfusion, and hyporeflectivity of the middle layer due to the development of atrophy.

In addition, Sridhar *et al.* proposed a classification for PAMM based on the patterns seen in en-face OCT and the presumed pathophysiological mechanism. The following three patterns were described: arteriolar, globular, and fern [5]. The arteriolar pattern showed band-like hyperreflectivity that corresponds to the distribution of a large retinal arteriole and is caused by a transient arteriole or true arteriolar occlusion. The globular pattern showed a focal ovoid patch or multifocal ovoid patches of hyperreflectivity of the middle retina caused by distal

CHAPTER 3

The Role of Macular Perfusion as a Contributing Factor in the Pathogenesis of Myopic Macular Traction Maculopathy

Miguel A. Quiroz-Reyes, MD[1,*], Erick A. Quiroz-Gonzalez[1,2], Margarita Montano[1], Miguel A. Quiroz-Gonzalez[1], Sanjay Marasini[3] and **Virgilio Lima-Gomez, MD[4]**

[1] *Oftalmologia Integral ABC, Retina Department, Medical and Surgical Assistance Institution (Nonprofit Organization), Affiliated with the Postgraduate Studies Division, National Autonomous University of Mexico, Mexico City, Mexico*

[2] *Institute of Ophthalmology, Fundacion Conde de Valenciana, Private Assistance Institution (Nonprofit Organization), Mexico City, Mexico*

[3] *Department of Ophthalmology, The University of Auckland, Auckland, New Zealand*

[4] *Ophthalmology Service, Hospital Juarez de Mexico, Public Assistance Institution (Nonprofit Organization), Mexico City, Mexico*

Abstract: Recently, qualitative and quantitative perfusional evaluations of vessel density (VD) and choriocapillaris flow patterns at the macular level have changed the evaluation spectrum and management of different macular pathologies. Published data on long-term macular perfusional findings and quantitative VD and flow evaluation (perfusion indices) in patients at different stages of successfully operated myopic traction maculopathy (MTM) compared with the corresponding values in normal control subjects are limited. This chapter describes the role of macular perfusion as a contributing factor to the pathogenesis of MTM.

The primary outcome measure included the long-term structural and perfusional macular status across groups. Forty-six eyes of 34 patients were included in the study group. The axial length was 29.89±1.67 mm. The postoperative follow-up period was 43±26.77 months. The preoperative BCVA was 1.29±0.54 logMAR, and the postoperative BCVA was 0.60±0.52 logMAR ($P<0.05$). The difference in perfusion indices across groups was statistically significant ($p<0.005$). Surgically resolved MTM eyes generally had a larger superficial foveal avascular zone area, lower vessel density, smaller choriocapillaris flow area (CFA), thinner central subfoveal thickness (CSFT),

* **Corresponding author Miguel A. Quiroz-Reyes, MD:** Oftalmologia Integral ABC, Retina Department, Medical and Surgical Assistance Institution (Nonprofit Organization), Affiliated with the Postgraduate Studies Division, National Autonomous University of Mexico, Mexico City, Mexico; Tel: +525 5217 2732; Fax: +525 55 1664 7180; E-mail: drquiroz@prodigy.net.mx and drquirozreyes7@gmail.com

and more macular defects. Better functional, structural, and perfusion index outcomes were observed in highly myopic eyes that underwent early surgery.

Keywords: Autologous retina grafting, Choriocapillaris flow area, Choriocapillaris subfoveal plexus, Deep vascular plexus, Foveal avascular zone, Foveoretinal detachment, High myopia, Myopic foveoschisis, Myopic macular degeneration, Myopic macular hole, Myopic macular hole-associated retinal detachment, Myopic traction maculopathy, Perfusion indices, Superficial vascular plexus, Vessel density.

INTRODUCTION

High myopia is a major cause of legal blindness in industrialized countries, and its prevalence has steadily increased over the last few decades. There is a myopia epidemic in East and Southeast Asia, with an estimated prevalence of 80–90% of the total population, of which approximately 10-20% of cases involve high myopia alone [1]. In the United States, it affects nearly 2% of the general population aged between 12 and 54 years [2]. Pathological myopia is the fifth leading cause of low vision or blindness in Japan, and the second leading cause among people older than 40 years of age in China [3].

Macular changes in patients with high myopia (spherical equivalent of -6.0 diopters or axial length greater than 26.5 mm) are characterized by retinal atrophy, ruptures in Bruch's membrane, and sclerotic thinning. Pathological myopia (PM) can be complicated by posterior staphyloma (PS) and macular atrophy [4]. In its early stages, myopic traction maculopathy (MTM), also called myopic foveoschisis (MF), is a schisis-like thickening of the retina. It has recently been described as tractional elongation of the Henle nerve fiber layer in eyes with high myopia and PS, rather than splitting of the retina [5, 6]. MF is more common in females [7, 8].

Scleral alterations have been proposed as the driving force of posterior segment pathologies. Scleral thinning and localized ectasia due to a reduction in the thickness of individual collagen fibers have been observed in myopic eyes [9, 10]. MF is a relatively new term that was first described by Panozzo and Mercanti [7] using optical coherence tomography (OCT) in terms of subtle macular changes, such as epiretinal membrane (ERM), vitreomacular traction (VMT), macular or foveal retinoschisis, retinal thickening, lamellar or partial-thickness macular hole, full-thickness myopic macular hole (MH) with or without retinal detachment, and PS. These scleral pathological alterations and subsequent increases in axial length may contribute to foveomacular retinoschisis, which exacerbates preexisting VMT. VMT is considered the cause of traction-related vitreoretinal interface

abnormalities such as ERMs, posterior cortex hyaloid remnants, and retinal vessel rigidity [5]. In addition, enhanced-depth OCT imaging has revealed choroidal thinning in the macular region to be the consequence of age-related degenerative changes [11, 12].

The most recent MTM classification and its corresponding staging were proposed by Parolini *et al.* [13, 14]. This system describes the evolution of four retinal stages (1–4) and three foveal stages (a–c). Stages 1 and 2 represent the earliest stages of MTM, while stages 3 and 4 are associated with macular hole and retinal detachment, respectively. Progression in the stages was correlated with a decrease in the best-corrected visual acuity (BVCA) [14]. The pathological significance of MTM is important to determine when to surgically treat these patients but is most critical for deciding when to treat the fellow eye [15]. MF, as the earliest stage of MTM, is defined as tractional elongation of the Henle nerve fiber layer and is present in approximately 9-34% of patients with PM [7, 16, 17]. The natural evolution of highly myopic eyes with macular or foveal retinoschisis and foveoretinal detachment (FRD) involves the development of MHs [18 - 20].

In some patients, early stage MTM remains stable for several years. However, in others, it progresses to FRD and MH, with subsequent visual impairment [5]. Tractional forces, when combined with PS, are important causes of these consequences [21]. The specific cause of foveoschisis is not yet fully understood. However, a few proposed mechanisms for its pathogenesis include axial traction generated by progressive elongation of the eyeball and subsequent stretching forces developing in the posterior retina. The premacular vitreous cortex with tangential traction may be secondary to the rigidity of the internal limiting membrane (ILM) and retinal vessels. All these degenerative changes may occur within the context of PS [5, 22, 23].

Current options for the treatment of MTM at different stages include a three-port pars plana vitrectomy (PPV) technique with modified fovea-saved ILM or without ILM peeling, foveal-sparing ILM, inverted-flap ILM peeling, inverting multi-layer ILM flap techniques, free-autologous ILM transplantation, and autologous retina grafting techniques with silicone oil or gas tamponade. Macular buckling has also been attempted with favorable results [15, 24 - 27]. The identification of the early stages is a major factor in deciding the management strategy. Vitrectomy with the release of vitreoretinal traction yields good results and visual recovery. However, some patients require multiple interventions to achieve anatomical and functional success. Early stage symptomatic MTM, such as foveoschisis, may progress to myopic FRD, partial-thickness MH and/or full-thickness MH without retinal detachment, and macular hole retinal detachment (MHRD) within the natural course of the disease [5, 15].

CHAPTER 4

Postoperative Ocular Perfusional Findings in Successfully Reattached Severe Proliferative Vitreoretinopathy, An OCT-A Evaluation

Juan Pablo Dávila-Gonzalez[1,*] and **José Dalma-Weiszhausz**[2]

[1] *Dalma y Asociados SC. Mexico City, Mexico*

[2] *Asociacion para prevenir la Ceguera en Mexico, Mexico City, Mexico*

Abstract: Rhegmatogenous retinal detachment (RRD) is the separation of the neurosensory retina from the underlying retinal pigment epithelium (RPE) and is one of the leading causes of severe vision loss when it involves the macula or proliferative vitreoretinopathy (PVR) in different stages. Optical coherence tomography (OCT) and Optical coherence tomography - angiography (OCT-A) have opened a new scenario in the investigation of macular microstructural abnormalities in RRD.

Findings in the preoperative retinal detachment structural B-scans in OCT such as ellipsoid zone (EZ)/external limiting membrane (ELM) integrity, cavities along the inner nuclear layer (INL) or outer nuclear layer (ONL), retinal height of detachment at the fovea, presence of retinal folds and subfoveal choroidal thickness may predict the functional and structural outcomes.

Structural and en-face analysis with OCT-A in RRD with PVR has demonstrated an enlarged foveal avascular zone, and changes in the flow at the superficial, intermediate and deep capillary plexus during 6 months postoperative follow up. High resolution and deep enhancing imaging OCT-A technology will provide an important role regarding the choriocapillaris and choroid and their potential correlation with visual acuity recovery.

OCT and OCT-A will provide preoperative prognostic biomarkers and adequate vascular retinochoroidal layers may influence a postoperative outcome.

Keywords: Angiography, Outer nuclear layer (ONL), Rhegmatogenous retinal detachment (RRD), Retinal morphology, Retinal pigment epithelium (RPE).

INTRODUCTION

Rhegmatogenous retinal detachment (RRD) is the separation of the neurosensory retina from the underlying retinal pigment epithelium (RPE). In normal eyes, the rate of RRD is approximately 5 per 100,000 people per year [1]. It often causes severe vision loss when it involves the macula or proliferative vitreoretinopathy

* **Corresponding author Juan Pablo Dávila-Gonzalez:** Dalma y Asociados SC. Mexico City, Mexico; Tel: +52 55 5540-3428; E-mail: juan_pablo_davila@doctor.com

(PVR) in different stages. The incidence of PVR ranges from 5.1 to 11.7%, and remains the most common cause of failed repair rhegmatogenous retinal detachment. The risk factors for PVR are well known pre, intra and postoperative clinical findings [1]. Retinal pigment epithelium (RPE) cells are the key factor triggering PVR development in addition to multiple inflammatory and proliferative factors that induce non-vascular fibrocellular epiretinal membrane, intraretinal membranes and subretinal bands proliferation and contraction. Histologically, PVR membranes may appear gliotic, fibrovascular or fibroglial. PVR is believed to form from inward migration and proliferation of glial cells normally present in the nerve fiber and ganglion cell layers. Aside from glial cells, PVR membranes may also contain fibroblast and RPE cells [1, 2].

Various treatments can be performed to reattach the retina, including vitrectomy, scleral buckling, a combination of the two, pneumatic retinopexy, laser or cryocoagulation or newer techniques like tissue adhesive or retinal autografts in addition to multiples tamponades like SF_6 or C_3F_8 gas or silicon oil tamponade extensively used in the presence of advanced PVR [1, 2].

However, even after successful anatomic reattachment, the functional results show a wide range of visual outcomes. Poor visual acuity, permanent functional damage, persistent metamorphopsia or color vision defects can remain after surgery. Factors that affect the visual outcomes include the macula-off RRD, preoperative visual acuity, age of the patient, duration of the detachment, extension of the detachment, concomitant choroidal detachment, any degree of PVR, vitreous hemorrhage along with other ophthalmic conditions such as preretinal membrane formation, macular cysts or holes, senile cataracts or glaucoma [1, 2].

Optical coherence tomography (OCT) is the most accurate method to image the macular structure. The utilization of OCT in clinical practice has dramatically increased the ability to diagnose vitreomacular abnormalities, providing subclinical information and allowing physicians to visualize, classify and monitor the vitreomacular interface, retina and choroid with better accuracy. Findings in the preoperative retinal detachment structural B-scans in OCT such as ellipsoid zone (EZ) / external limiting membrane (ELM) integrity, cavities along the inner nuclear layer (INL) or outer nuclear layer (ONL), retinal height of detachment at the fovea, presence of retinal folds and subfoveal choroidal thickness may predict the functional and structural outcomes [3, 4].

In the last decades, the use of fluorescein angiography has revealed abnormalities in the retinal perfusion of patients with RRD. Some findings include vascular dilation and hyperpermeability because of tissue hypoxia [5].

Emerging evidence using OCT-Angiography (OCT-A), a new imaging technology represents one of the latest revolutions in retinal imaging.

OCT-A has opened a new scenario in the investigation of macular microstructural abnormalities in RRD. OCT-A has revealed the existence of microscopic macular changes, even in cases where retinal morphology appears normal on the fundus biomicroscopy. Despite the increased rate of successful anatomical retinal reattachment after surgery in non-complicated or complicated RDD, a substantial proportion of patients have unexpected limited visual outcomes, indicating that the functional status of the macula may not be entirely restored. It is possible that circulatory changes at the macular capillary level may explain this low visual recovery. The microcirculation system of the macula consists of retinal and choroidal capillary networks. The superficial capillary plexus (SCP) and the deep capillary plexus (DCP) are located within the ganglion cell layer and the inner nuclear layer, respectively. They are responsible for providing nourishment to the inner retinal layer and removing metabolic products. The intermediate capillary plexus (ICP), located in between the SCP and DCP, is a distinct vascular network whose formation seems to depend more on hypoxia-induced factors than the other capillary plexus [5 - 8].

Macular microvascular disturbance has been previously shown to be present in RRD eyes even without macular involvement. Scanning-laser doppler flowmetry has shown macular flow velocity decrease, probably due to an autoregulation phenomenon secondary to tissue hypoxia [7].

There is little quantitative analysis information considering the association between OCT-A characteristics and the final visual acuity in RRD and PVR after successful surgery. Changes in the macular capillary plexus after RRD may indicate the presence of ischemic damage in the fovea leading to poor visual outcomes. The first analysis of OCT-A characteristics after RRD surgery was published by Sato and colleagues in 2017, who demonstrated, in 22 eyes, no association of FAZ area changes with the SCP and DCP with visual acuity (VA) at 1, 3 and 6 months after vitrectomy. In 2018, Woo and co-authors published 34 cases with and without macular involvement and found that both superficial and especially deep FAZ were markedly larger in the macula-off after 2 months. In addition, DCP flow deficit was affected probably due to the watershed zone and lower oxygen saturation, making this deep plexus more vulnerable to hypoxia compared to the SCP directly related to large retinal arterioles, which have higher perfusion pressure. Patients with macula-on postoperative FAZ were not significantly different from the control group, so changes in FAZ observed may indicate ischemic changes leading to suboptimal visual recovery. Observations by Yui and co-authors in some patients with RDD and PVR suggest that preoperative

CHAPTER 5

Polypoidal Choroidal Vasculopathy and Pachychoroid Neovasculopathy Represent Different Manifestations of the Same Disease

Erick A. Quiroz-Gonzalez[1,2,*], Miguel A. Quiroz-Reyes, MD[1] and **Zixuan Shao[3]**

[1] *Oftalmologia Integral ABC, Retina Department, Medical and Surgical Assistance Institution (Nonprofit Organization), Affiliated with the Postgraduate Studies Division, National Autonomous University of Mexico, Mexico City, Mexico*

[2] *Institute of Ophthalmology, Fundacion Conde de Valenciana, Private Assistance Institution (Nonprofit Organization), Mexico City, Mexico*

[3] *Division of Chemistry and Chemical Engineering, California Institute of Technology, Pasadena, CA, USA*

Abstract: The pachychoroid spectrum has various clinical manifestations. There are three major characteristics, all of which have an unknown etiology and controversial pathogenesis: pachychoroid, presence of pachyvessels at the external choroid, and inner choroidal attenuation. This study describes a patient with clinical and multimodal manifestations in the pachychoroid spectrum, in which different clinical variants are presented in both eyes simultaneously. Specifically, the patient had an acute visual loss and massive hemorrhagic maculopathy in the right eye, and a chronic decrease in visual acuity and metamorphopsia in the left eye accompanied by pigmentary changes and subretinal fluid at the geometric center of the fovea. The patient underwent a complete ophthalmological examination and multimodal imaging and was diagnosed with polypoidal choroidal vasculopathy (PCV) and pachychoroid neovasculopathy (PNV); two different manifestations of the same disease spectrum occur simultaneously.

Owing to the active nature of the disease, the patient received three doses of intravitreal antiangiogenic agents in each eye. Many different degenerative etiologies have been considered, such as pathological choroidal neovascularization due to age-related macular degeneration (AMD) and pachychoroid spectrum. Evaluation of the choroid vasculature using swept-source optical coherent tomography (SS-OCT) and OCT angiography (OCT-A) revealed the origin of the disease to be idiopathic. PCV and PNV are considered to represent a single end-stage of the pachychoroid spectrum with

* **Corresponding author Erick A. Quiroz-Gonzalez:** Oftalmologia Integral ABC, Retina Department, Medical and Surgical Assistance Institution (Nonprofit Organization), Affiliated with the Postgraduate Studies Division, National Autonomous University of Mexico, Mexico City, Mexico; E-mail: erwick-andrew@hotmail.com

Miguel A. Quiroz-Reyes and Virgilio Lima-Gomez (Eds.)

different manifestations; the former presents with aneurysmatic characteristics, whereas the latter lacks this anomaly.

Keywords: Central serous chorioretinopathy, Choroidal neovascularization, Hemorrhagic maculopathy, Pachychoroid neovasculopathy, Pachychoroid spectrum, Peripapillary pachychoroid syndrome, Pachychoroid neovasculopathy polypoidal choroidal vasculopathy, Polypoidal choroidal neovascularization, Retinal angiomatous proliferation.

INTRODUCTION

The pachychoroid spectrum comprises several manifestations of a single disease [1]. The word pachychoroid is derived from Greek, meaning “thick” choroid. Three major characteristics are associated with the pachychoroid spectrum. First, although there is no precise cutoff point of choroidal thickness for diagnosis (probably due to physiological fluctuations influenced by the circadian cycle, blood pressure, hydration status, sex, axial length, and other factors [2]), recent studies have reported that a thickness of >270-300 microns indicates the presence of pachychoroid [3, 4]. Second, pachyvessels or a dilated Haller’s plexus cause compression of the Sattler’s plexus and choriocapillaris, decreasing the oxygen concentration at the Ruysch’s complex (retinal pigment epithelium (RPE), Bruch’s membrane, and choriocapillaris). Third, inner choroidal attenuation has also been observed in this disease [5].

The etiology of pachychoroid disease is not well understood; however, both exogenous and endogenous factors (including genetic background) are likely involved. Some reports point to choroidal congestion as a possible contributor to disease progression [6], yet the exact pathogenesis remains controversial. Additionally, mineralocorticoid and corticosteroid receptors are abundantly expressed in the choroidal vasculature, contributing to the increase in choroidal thickness [4, 7] and functional anomalies secondary to hydrostatic pressure alteration [8]. Altogether, these three main characteristics, in particular, the attenuation of choriocapillaris, lead to retinal pigment epithelium (RPE) dysfunction, photoreceptor atrophy, and subsequent development of choroidal neovascularization (CNV) in response to significant choroidal ischemia [5, 9] and sub-RPE endothelial cell proliferation due to pigmentary epithelium detachments (PEDs) [10].

The pachychoroid spectrum comprises central serous chorioretinopathy (CSC), pachychoroid pigment epitheliopathy (PPE), polypoidal choroidal vasculopathy (PCV), pachychoroid neovasculopathy (PNV), focal choroidal excavation (FCE), and peripapillary pachychoroid syndrome (PPS) [2, 7]. PCV has been described as

an area of choroidal vasculature proliferation immediately beneath the RPE, forming a branching vascular network (BVN) with edges exhibiting vascular dilatations or aneurysms, controversially named polyps, because this word refers to dilatation of a mucous membrane, and it is more accurate to use the term aneurysm instead of polyp, as proposed by the CONAN group [11]. The presence of this aneurysmatic lesion develops serous or hemorrhagic PEDs and evolves into massive hemorrhagic maculopathy with areas of lipid exudation [7] (Fig. **1**).

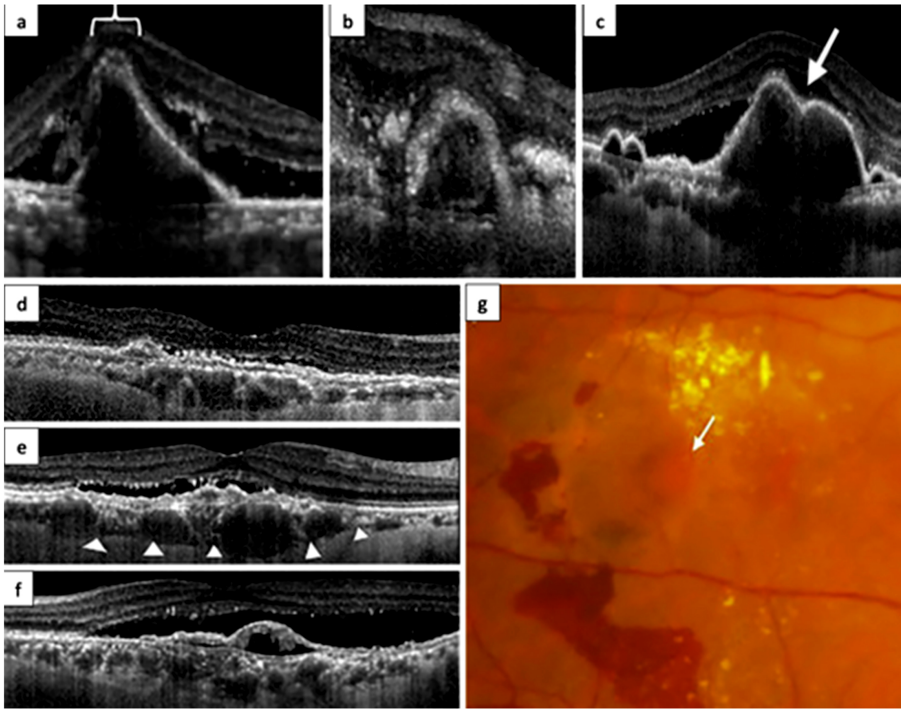

Fig. (1). Reference images for 7 selected features evaluated for inclusion into the final set of polypoid choroidal vasculopathy diagnostic criteria. (**a**) Sharp-peaked pigment epithelial detachment (PED). (**b**) Subretinal pigment detachment ring-like lesion. (**c**) Complex or multilobular PED (arrow highlighting the notch within the outline of the PED). (**d**), Double-layer sign or shallow, irregular retinal pigment epithelium (RPE) elevation. (**e**), Thick choroid with dilated Haller's layer vessels (scleral choroidal interface shown by arrowheads). (**f**), Predominance of subretinal fluid and Complex RPE elevation observed with in OCT. (**g**) Orange nodule (white arrow). This modified multipanel figure was originally published by the Asia-Pacific Ocular Imaging Society PCV Workgroup. Ophthalmology 2021; 128:443-452 by the American Academy of Ophthalmology.

This disease is classified as a variant of age-related macular degeneration (AMD), and many authors believe that 1 in 10 pachychoroid patients is misdiagnosed with neovascular AMD [2, 12], particularly when choroidal imaging is not performed [13]. PNV can be considered the final stage of CSC or PPE due to type 1 CNV formation, leading to chronic disease and subsequent photoreceptor destruction. In

CHAPTER 6

The Current Role of OCTA in the Management of Pathological Choroidal Neovascularization with Anti-VEGF Therapy

Miguel A. Quiroz-Reyes, MD[1,*], Zixuan Shao[2] and **Erick A. Quiroz-Gonzalez[1,3]**

[1] *Oftalmologia Integral ABC, Retina Department, Medical and Surgical Assistance Institution (Nonprofit Organization), Affiliated with the Postgraduate Studies Division, National Autonomous University of Mexico, Mexico City, Mexico*

[2] *Division of Chemistry and Chemical Engineering, California Institute of Technology, Pasadena, CA, USA*

[3] *Institute of Ophthalmology, Fundacion Conde de Valenciana, Private Assistance Institution (Nonprofit organization), Mexico City, Mexico*

Abstract: Optical coherence tomography angiography (OCT-A) is an emerging technology that captures flow motion within the retinal vasculature to produce angiograms. Compared to dye-based angiography techniques, OCTA is a noninvasive and fast method that enables detailed visualization of the vasculature, which is not easily observable using previously available techniques. Over the past decade, OCT-A has been used to characterize the pathological features of choroidal neovascularization (CNV) associated with several retinal diseases, including neovascular age-related macular degeneration (AMD). In eyes at risk of developing CNV, OCT-A has demonstrated the capability to detect subclinical signs of neovascularization (NV) that may enable early treatment and better visual outcomes. Various CNV conditions are now routinely treated with intravitreal injections of anti-vascular endothelial growth factor (anti-VEGF). OCT-A was used to identify the characteristics of CNV at various stages, before and after anti-VEGF therapy. Although preliminary, OCT-A has demonstrated the potential to help guide treatment decisions in CNV cases that respond differently to anti-VEGF therapy.

Despite its multiple advantages and applications, the clinical use of OCT-A remains limited. OCT-A has several limitations, including visualization of a small area, the presence of artifacts, and results that are challenging to interpret. However, OCTA technology continues to advance as some of the early limitations have been resolved. Overall, OCT-A promises to be a significant step forward in our current ability to

[*] **Corresponding author Miguel A. Quiroz-Reyes, MD:** Oftalmologia Integral ABC, Retina Department, Medical and Surgical Assistance Institution (Nonprofit Organization), Affiliated with the Postgraduate Studies Division, National Autonomous University of Mexico, Mexico City, Mexico; Tel.: +52 55 5217 2732; Fax: +52 55 1664 7180; E-mails: drquiroz@prodigy.net.mx and drquirozreyes7@gmail.com

Miguel A. Quiroz-Reyes and Virgilio Lima-Gomez (Eds.)

visualize pathological CNV, and has the potential to improve both the diagnosis and management of a variety of retinal diseases.

Keywords: Age-related macular degeneration, Anti–vascular endothelial growth factor, Myopic choroidal neovascularization, Central serous chorioretinopathy, Choroidal neovascularization, Geographic atrophy, Ischemic macula, Optical coherence tomography angiography, Pathological choroidal neovascularization, Type I and Type II choroidal neovascularization, Vascular endothelial growth factor.

INTRODUCTION

Choroidal neovascularization (CNV) is characterized by abnormal blood vessel growth from the choroidal vasculature through Brunch's membrane into the retina. The majority of CNV cases are observed in neovascular age-related macular degeneration (AMD); however, CNV can also be found in numerous other conditions, including myopic degeneration, chronic central serous chorioretinopathy, and choroidal tumors. CNV consists of clusters of ill-developed immature vessels that are prone to fluid leakage, leading to retinal edema and hemorrhage that subsequently cause a rapid decline in visual function. Among the biological factors involved in this process, the vascular endothelial growth factor (VEGF) plays a central role in stimulating and sustaining pathological angiogenesis in the retina [1]. Thus, targeting VEGF has become a central strategy in the treatment of multiple retinal conditions characterized by abnormal angiogenesis and fluid exudation.

CNV is currently routinely managed by anti-VEGF drugs that have largely replaced earlier treatment options such as laser photocoagulation and photodynamic therapy [2]. Anti-VEGF drugs are typically administered via intravitreal injection into the vitreous, whereas the more recent approval of Susvimo provides a refillable, implantable delivery option with slow drug release for up to six months [3]. Mechanistically, anti-VEGF blocks the activity of VEGF protein to reduce fluid leakage and rescue vision loss. However, continued treatment is needed to optimize visual outcomes, and cases with persistent fluid despite intervention are frequently observed [1].

Optical coherence tomography (OCT) was first developed in the early 1990s and is currently widely used for the diagnosis and management of retinal diseases [4]. OCT's popularity of OCT can be attributed to its non-invasive characteristics while simultaneously capturing high-resolution, cross-sectional images of the retina and surrounding tissues. These characteristics make OCT particularly

valuable in diagnosing retinal diseases where microscopic observation of the tissue through biopsy is not available [5].

In principle, OCT images are obtained by casting light that is divided into reference and sample beams to obtain a reflectivity versus depth profile for the retina. Specifically, the retina backscatters light waves, which interfere with the reference beam and create interference patterns that can be used to derive the light echoes versus the depth profile of the retina *in vivo* [4].

OCT technology has evolved substantially over the past three decades since its introduction. The initial instruments available used time-domain OCT technology (TD-OCT) technology, which has a very slow imaging speed and poor image quality [5]. It was not until the introduction of the first commercially available spectral domain OCT (SD-OCT) in 2006 that the adaptation of OCT truly took off [6]. SD-OCT uses a Fourier domain detection technique and improves TD-OCT with substantial upgrades in both imaging speed and image quality, reaching a level of detail that parallels histopathology [7].

Swept-source OCT (SS-OCT) is another modern OCT technology that uses a Fourier domain detection technique [5]. Unlike SD-OCT, which utilizes a near-infrared broadband light source and a combination of a spectrometer and a high-speed line-scan camera as the detector system, SS-OCT uses a rapidly sweeping tunable laser and a point photodetector as the detector [5, 8]. Compared to SD-OCT, SS-OCT is much faster in scan acquisition, reaching speeds of up to 400 thousand A-scans/second, which enables longer B-scans for widefield imaging [9, 10]. Additionally, SS-OCT platforms use a light source centered at a longer wavelength than SD-OCT (1050 nm *vs.* 840 nm in SD-OCT), allowing better tissue penetration and clearer visualization of the choroid and lamina cribrosa. However, longer wavelengths also reduce the image resolution, which becomes more severe in certain cases, such as in the presence of a thickened choroid or drusen. Additionally, SD-OCT's ability to image the outer retina can be improved with enhanced depth imaging (EDI) technologies that are available in all modern machines. Overall, the current rate of adoption of SS-OCT remains limited, mainly because of its high cost and lack of clear advantages over SD-OCT [11].

First commercialized in 2014, OCT angiography (OCT-A) is a relatively new technology that captures flow motion within the retinal and choroidal vasculature without using conventional contrast agents [12]. Unlike standard structural OCT, OCTA analyzes temporal changes in the OCT signal in addition to reflected light [13]. Through repeated B-scans at the same retinal location, OCT-A can isolate the temporal scattering changes caused by erythrocytes moving through vessels, and use the resultant fluctuation in the OCT signal to generate angiographic

CHAPTER 7

Epiretinal Membrane Formation and Macular Perfusion Findings in Rhegmatogenous Retinal Detachment Treated with Vitrectomy or Scleral Buckling

Miguel A. Quiroz-Reyes, MD[1,*], Erick A. Quiroz-Gonzalez[1,2], Miguel A. Quiroz-Gonzalez[1], Jorge Morales-Navarro[2], Felipe Esparza-Correa[2], Jorge E. Aceves-Velazquez[2], Jennifer H. Kim-Lee[2], Alejandra Nieto-Jordan[2], Margarita Montano[1], Sanjay Marasini[3] and **Virgilio Lima-Gomez, MD[4]**

[1] *Oftalmologia Integral ABC, Retina Department, Medical and Surgical Assistance Institution (Nonprofit Organization), Affiliated with the Postgraduate Studies Division, National Autonomous University of Mexico, Mexico City, Mexico*

[2] *Institute of Ophthalmology, Fundacion Conde de Valenciana, Private Assistance Institution (Nonprofit Organization), Mexico City, Mexico*

[3] *Department of Ophthalmology, The University of Auckland, Auckland, New Zealand*

[4] *Ophthalmology Service, Hospital Juarez de Mexico, Public Assistance Institution (Nonprofit Organization), Mexico City, Mexico*

Abstract: Despite the abundant literature on management options for noncomplicated macula-off rhegmatogenous retinal detachment (RRD) repair, the role of the corresponding long-term postoperative macular perfusion indices and their correlation with the postoperative epiretinal membrane (ERM) formation remain vaguely understood. In this chapter, we have analyzed the incidence of postoperative ERM proliferation and the differences in the corresponding postoperative macular perfusion indices in patients who underwent two well-known surgical approaches for noncomplicated macula-off RRD. Postoperative microstructural and perfusional findings were compared, and their correlation with best-corrected visual acuity (BCVA), postoperatively, was assessed. Two study groups based on the surgical procedures performed for noncomplicated macula-off RRD were analyzed. The postoperative incidence of ERM was 23.2% and 23.63% in the buckle vitrectomy groups, respectively ($p>0.05$). The RRD recurrence rates in the buckle and vitrectomy groups were 8.8% and 1.82%, respectively ($p>0.001$). The mean BCVA values before ERM removal in the buckle and vitrectomy groups were 0.40±0.33 log of the minimum

* **Corresponding author Miguel A. Quiroz-Reyes, MD:** Oftalmologia Integral ABC, Retina Department, Medical and Surgical Assistance Institution (Nonprofit Organization), Affiliated with the Postgraduate Studies Division, National Autonomous University of Mexico, Mexico City, Mexico; Tel: +52 55 5217 2732; Fax: +52 55 1664 7180; E-mails: drquiroz@prodigy.net.mx and drquirozreyes7@gmail.com

angle of resolution (logMAR) and 0.47±0.19 logMAR, respectively ($p<0.05$). The final mean postoperative BCVA in the buckle and vitrectomy groups were 0.43±0.14 logMAR and 0.28±0.19 logMAR, respectively ($p<0.05$). When the retinal perfusional indices of the buckle and vitrectomy groups were compared with the normal control group, all the perfusional indices differed significantly ($p<0.01$).

Keywords: Additional surgery rate, Brilliant blue dye, Choriocapillaris flow area, Deep vascular plexus, Ellipsoid zone, Epiretinal membrane, External limiting membrane, Internal limiting membrane, Macula-off retinal detachment, Noncomplicated rhegmatogenous retinal detachment, Primary vitrectomy, Scleral buckle, Superficial vascular plexus, Vessel density.

INTRODUCTION

Several complications may occur during scleral buckle surgery to manage primary noncomplicated macula-off rhegmatogenous retinal detachment (RRD) [1]. These complications may include vitreoretinal complications, retinal perforation with vitreoretinal entrapment, choroidal hemorrhage, and subretinal bleeding [1]. One of the most commonly observed postoperative complications after scleral buckling and cryotherapy surgery is macular ectopia due to vitreomacular traction and proliferative vitreoretinopathy (PVR) with recurrent and complicated RRD along with epiretinal membrane (ERM) proliferation [1, 2].

Data from a recent (2022) meta-analysis of 7212 eyes showed that the scleral buckle offers a slightly higher final reattachment rate and a reduced risk of macular edema and cataract in cases of RRD [3]. However, the historical data reveal that primary vitrectomy is the preferred procedure for noncomplicated RRD as it reduces complications. Poulsen *et al.* [4] reported that approximately 36% macular attachment was achieved after pars plana vitrectomy (PPV) in primary RRD, and most of the patients achieved a reasonable long-term visual outcome. However, the incidence of ERM is high. To prevent the development of ERM and the requirement of additional surgeries, many surgeons opt to remove the internal limiting membrane (ILM) at the time of PPV while managing RRD. However, the removal of the ILM may lead to the proliferation of glial and Müller cells, which exert a tangential contraction over the macula [5, 6]. Therefore, the potential benefits of prophylactic ILM removal are controversial [7 - 11].

Over the last decade, retinal imaging has progressed significantly, facilitating an accurate assessment of anatomical, vascular and functional outcomes before and after retinal surgery. Recent studies have shown that after vitreoretinal surgeries, early microvascular alterations in the retina can be observed and quantified to monitor and predict surgical outcomes. Optical coherent tomography angiography (OCT-A) devices have allowed a detailed analysis of the retina and

choriocapillaris in the macular retina in different pathologic conditions and highlighted distinct changes [12]. Therefore, assessing perfusional indices after vitreoretinal surgeries, including primary scleral buckle placement and primary vitrectomy, would allow us to make future surgical decisions for better anatomical and functional outcomes.

Methodology and Chapter Design

This chapter aims to elaborate on the postoperative outcomes in two surgical groups. The objectives were to 1) determine the postoperative comparative incidence of ERM proliferation, 2) analyze the long-term final postoperative structural findings using optical coherence tomography (OCT), 3) correlate the final postoperative best-corrected visual acuity (BCVA) with the two types of surgical procedures in cases of uncomplicated macula-off RRD, and 4) compare the perfusional indices between the buckling group and vitrectomy group to those of the control emmetropic group to explore potential microvascular alterations (Table **1**).

To analyze structural and perfusional findings, complications were identified associated with scleral buckle and vitrectomy with a complementary buckle. All vitrectomy eyes on which a complementary scleral buckle was placed were not included in this analysis.

Table 1. Study groups. The anatomical and functional outcomes of the groups were compared to evaluate trans- and postoperative complications [7].

Study groups	Group characteristics
Buckle group	Noncomplicated primary RRD eyes without preoperative ERM proliferation and that were managed using 360° scleral buckle surgery, and rhegmatogenous lesions limited cryotherapy retinopexy or additional subretinal fluid exo-drainage
Vitrectomy group	Noncomplicated primary RRD eyes without evidence of preoperative ERM proliferation that underwent primary vitrectomy with no ILM removal

The SD-OCT and OCT-A findings were compared with the emmetropic control groups to identify any potential alterations after the surgeries. The dataset analyzed was taken from a previous report by the authors [7] (Figs. **1** and **2**).

CHAPTER 8

OCT-A Findings and Usefulness in Alzheimer's Disease, Parkinson's Disease, and Systemic Lupus Erythematosus

Sanjay Marasini[1] and **Miguel A. Quiroz-Reyes, MD**[2,*]

[1] *Department of Ophthalmology, The University of Auckland, Auckland, New Zealand*

[2] *Oftalmologia Integral ABC, Retina Department, Medical and Surgical Assistance Institution (Nonprofit Organization), Affiliated with the Postgraduate Studies Division, National Autonomous University of Mexico, Mexico City, Mexico*

Abstract: The eye is a window to the brain because of its inherent connection to the central nervous system (CNS). Several brain disorders manifest as ophthalmic abnormalities and can be detected through a detailed assessment of the eyes. In the last decade, extensive evaluation of retinal microvascular changes using optical coherence tomography angiography (OCT-A) has been performed for several diseases, such as Parkinson's disease, Alzheimer's disease, and systemic lupus erythematosus. Although the results from the available studies are conflicting (mainly due to heterogeneous study populations), they agree on the applicability of this technology for the early identification of these diseases. This chapter summarizes the OCT-A screening and monitoring uses for these diseases and hypotheses for the potential identification of disease characteristics.

Keywords: Alzheimer's disease, Autoimmune diseases, Binarization, Cognitive impairment, Foveal avascular zone, Fundus fluorescein angiography, Hydroxychloroquine, Macular perfusion, Neurodegenerative diseases, Optical Coherent Topography, Optical Coherence Tomography Angiography, Parkinson's disease, Perfusion density, Retinal vessel density, Perfusion density, Retinal thinning, Skeletonization, Systemic Lupus Erythematosus, Vascular perfusion indices, Vessel density.

[*] **Corresponding author Miguel A. Quiroz-Reyes, MD:** Oftalmologia Integral ABC, Retina Department, Medical and Surgical Assistance Institution (Nonprofit Organization), Affiliated with the Postgraduate Studies Division, National Autonomous University of Mexico, Mexico City, Mexico; Tel.: +52 55 217 2732; Fax: +52 55 1664 7180; E-mails: drquiroz@prodigy.net.mx and drquirozreyes7@gmail.com

Miguel A. Quiroz-Reyes and Virgilio Lima-Gomez (Eds.)

INTRODUCTION

The eye is referred to as a window to the brain because of its inherent connection to the central nervous system. Several brain disorders (*e.g.,* brain tumors) affect eye function; therefore, a detailed anatomical and physiological assessment of the eyes can help diagnose these disorders. The correct diagnosis of neurodegenerative brain diseases, such as Parkinson's disease and Alzheimer's disease, is especially challenging. Approximately 25% of the cases are diagnosed incorrectly, even in developed countries [1]. Expanding the knowledge base for these conditions' heterogeneous clinical presentations has helped identify newer methods to diagnose these conditions. Genetic testing, histopathological testing, olfactory testing, magnetic resonance imaging (MRI), and computed tomography imaging are currently used to diagnose most brain disorders. However, these methods are invasive, costly, and time consuming. Therefore, non-invasive cost-effective methods that can help diagnose such diseases are currently under investigation. One such emerging technique is optical coherence tomography angiography (OCT-A), which provides noninvasive detailed numerical quantification of microvascular perfusion of the retina (which is known to be affected by neurodegenerative diseases). Optical coherence tomography (OCT) measurements of the retina have revealed several valuable diagnostic findings in neurodegenerative diseases. However, their diagnostic power is limited because of the overlap in OCT changes seen in neurodegenerative diseases and prevalent ophthalmological diseases such as glaucoma, diabetic retinopathy, and age-related macular degeneration [2]. Therefore, the integration of vascular perfusion parameters, such as microvascular perfusion density, vessel calibers, and alterations in vascular network organization, may increase the diagnostic accuracy of these conditions. Therefore, these parameters can be measured using OCT-A and have the potential to be developed as indicators of brain disease [2].

First used to image the retina in 1991 [3], OCT-A technology has made a significant leap in disease diagnosis in recent years, especially for its use in en face visualization of the retinal circulation into anatomic slabs of the superficial and deep vascular networks that supply the various retinal layers [4]. OCT-A essentially captures the backscattering of light between constantly moving red blood cells and a static neurosensory retina without the use of a dye. These images approach histology-level resolution, which shows the potential of detecting early microvascular pathological changes in patients *in vivo* [5]. Vascular pathology in retinal diseases (such as diabetic retinopathy, uveitis, retinal arterial occlusion, and retinal venous occlusions) can be assessed through quantitative analysis of anatomical markers using OCT-A, which makes it easier to compare pathologies. These analyses included vessel and perfusion densities, representing the percentage of blood vessels occupying a given area following image binarization

and skeletonization. OCT-A also allows the mapping of important clinical findings such as macular telangiectasia, impaired perfusion, microaneurysms, and capillary modelling [5]. OCT-A has been extensively used to evaluate its effectiveness in diagnosing the clinical and subclinical stages of several brain diseases and monitoring their progression.

OCT-A Technology

Detailed descriptions of the types and uses of OCT-A systems are beyond the scope of this book chapter, and readers are referred to a recent review by Lains *et al.* [6] for a more extensive understanding of OCTA application for retinal conditions. For practical guidance on OCT-A interpretations, readers are referred to the publication by Greig *et al.* [7] and the assessment of the anterior segment by Lee *et al.* [8].

Conventional structural OCT aids clinicians in visualizing the anatomical changes that affect vision, but it does not offer information on the differences between small blood vessels and static tissue in most retinal layers [9]. As a result, OCT does not provide important information regarding vascular changes, such as capillary dropout or pathologic blood vessels in the retina [9]. In contrast, OCT-A employs motion contrast imaging to generate high-resolution volumetric blood flow information to generate angiographic images within seconds that provide both structural and functional information. This method aims to contrast blood vessels from static tissues by assessing the change in the OCT signal caused by flowing blood cells [9]. OCT-A compares the decorrelation signal (differences in the backscattered OCT signal intensity or amplitude) between sequential OCT b-scans taken at precisely the same cross-section to construct a map of blood flow. Axial bulk motion from patient movement is eliminated; therefore, sites of motion between repeated OCT b-scans represent strict erythrocyte movement in retinal blood vessels [10]. Each three-dimensional scan takes approximately six seconds to obtain. OCT angiograms can then scroll outward from the internal limiting membrane to the choroid to visualize the individual vascular plexus and segment the inner retina, choriocapillaris, or other areas of interest [10]. With developments in OCT system speeds owing to better hardware, methods for OCT-A have shifted from comparing adjacent A-scans to sequential cross-sectional B-scans. This ensured that a slower flow in the microvasculature could be detected [9]. However, leakage information cannot be appreciated, and the exact size and location can be measured for pathologies, such as choroidal neovascularization.

This chapter focuses on the use of OCT-A technology for neurological diseases.

Systemic lupus erythematosus (SLE), a chronic autoimmune inflammatory disease, is of interest to ophthalmologists owing to its association with the eye.

CHAPTER 9

Branch and Central Retina Artery Occlusion and its treatment according to OCT-A Findings

Geraint J. Parfitt[1] and **Miguel A. Quiroz-Reyes, MD**[2,*]

[1] *School of Optometry & Vision Sciences, Cardiff University, Cardiff, United Kingdom*

[2] *Oftalmologia Integral ABC, Retina Department, Medical and Surgical Assistance Institution (Nonprofit Organization), Affiliated with the Postgraduate Studies Division, National Autonomous University of Mexico, Mexico City, Mexico*

Abstract: The retina requires a large blood supply to cope with the metabolic demands of the tissue, so it is vulnerable to hypoxia when the arterial blood flow is obstructed. Retinal artery occlusions are not common, but they can cause severe vision loss and may be indicative of cardiovascular disorders, such as cerebral stroke and ischemic heart disease. The central retinal artery arises from the ophthalmic artery and its branches supply blood to the inner retina via the superficial capillary plexus. Central retinal artery occlusion (CRAO) is characterized by an obstruction to the central retinal artery that often presents with severe vision loss and a poor prognosis. Branch retinal artery occlusion (BRAO) is defined by a blockage of a branch of the central retinal artery, which typically has a good prognosis if visual acuity is 20/40 or better on presentation. Optical coherence tomography-angiography (OCT-A) is a rapid, high-resolution imaging technique that can visualize the microvasculature of the retinal layers, including the superficial and deep capillary plexuses.

Therefore, it is possible to determine the microvascular changes that occur following retinal artery occlusions, and before and after potential therapies that are being actively researched. Therapies under investigation for the treatment of CRAO and BRAO include hyperbaric oxygen, fibrinolysis, and embolysis with laser therapy. In this chapter, the capabilities of OCT-A imaging to visualize and quantify retinal microvascular changes following CRAO and BRAO are assessed. Moreover, the use of OCT-A to understand the benefit of potential therapies is reviewed.

Keywords: Retinal artery occlusion, Optical coherence tomography angiography, Retinal vascular disease, Retinal ischemia.

[*] **Corresponding author Miguel A. Quiroz-Reyes, MD:** Oftalmologia Integral ABC, Retina Department, Medical and Surgical Assistance Institution (Nonprofit Organization), Affiliated with the Postgraduate Studies Division, National Autonomous University of Mexico, Mexico City, Mexico; Tel: +52 55 5217 2732; Fax: +52 55 1664 7180; E-mails: drquiroz@prodigy.net.mx and drquirozreyes7@gmail.com

Miguel A. Quiroz-Reyes and Virgilio Lima-Gomez (Eds.)

INTRODUCTION

The central retinal artery (CRA) branches from the ophthalmic artery, which stems from the internal carotid artery, to supply blood to the inner retina layers. The inner retina is composed of the retinal nerve fiber layer, ganglion cell layer, inner plexiform layer, and inner nuclear layer, whereas the outer retina contains the photoreceptor layers, retinal pigment epithelium, and choroid. The outer retinal layers are supplied by choroidal blood vessels that form the choriocapillaris that directly underlies Bruch's membrane and the retinal pigment epithelium. The CRA travels within the dural sheath of the optic nerve and upon reaching the posterior pole, it bifurcates into two main branches (superior and inferior), which further divide into the temporal and nasal branches that supply the retinal quadrants. Embedded in the ganglion cell layer is the superficial capillary plexus (SCP), which is supplied by the CRA. The SCP is connected by anastomoses to the intermediate capillary plexus (ICP), and deep capillary plexus (DCP), which supply blood to the other inner retinal layers, including the inner nuclear layer.

Central retinal artery occlusion (CRAO) is defined as the sudden obstruction of the central retinal artery, whereas branch retinal artery occlusion (BRAO) is an occlusion of a CRA branch. Retinal artery occlusion and obstructed blood flow into the retina can cause retinal ischemia and edema that leads to tissue atrophy and vision loss. Retinal ischemia subsequently causes a loss of retinal cell viability and atrophy of photoreceptors, which results in visual defects. BRAO is restricted to the region that is supplied by the occluded vessel and the extent of vision loss correlates with the size of the area affected by the obstructed blood vessel. On the other hand, CRAO is a type of acute ischemic stroke that often causes severe vision loss of 20/400 or worse and has a poor prognosis. Both types of retinal artery occlusion are an indicator of increased risk of cerebral stroke and ischemic heart disease [1], therefore, it requires careful assessment and referral to a stroke center.

Retinal artery occlusion can be a result of embolism, thrombosis, or increased intraocular pressure and may be temporary. Damage to the affected area can occur in minutes, even when the blood flow has been restored after the initial occlusion. CRAO can result in ischemic necrosis, whitening, and opacification of the inner retina, which may last for days and cause a cherry-red spot at the fovea. Moderate retinal artery occlusions can go unnoticed when there is not a significant level of retinal opacification [2].

As outlined in Chapter 1, optical coherence tomography – angiography (OCT-A) is a non-invasive imaging approach that can generate high-resolution images of

the retinal microvasculature to aid with the diagnosis and management of vascular disease, including retinal artery occlusion (Fig. **1**). OCT-A imaging can rapidly generate high-resolution cross-sections of the macula, which allows the clinical course of CRAO to be readily tracked over the long-term.

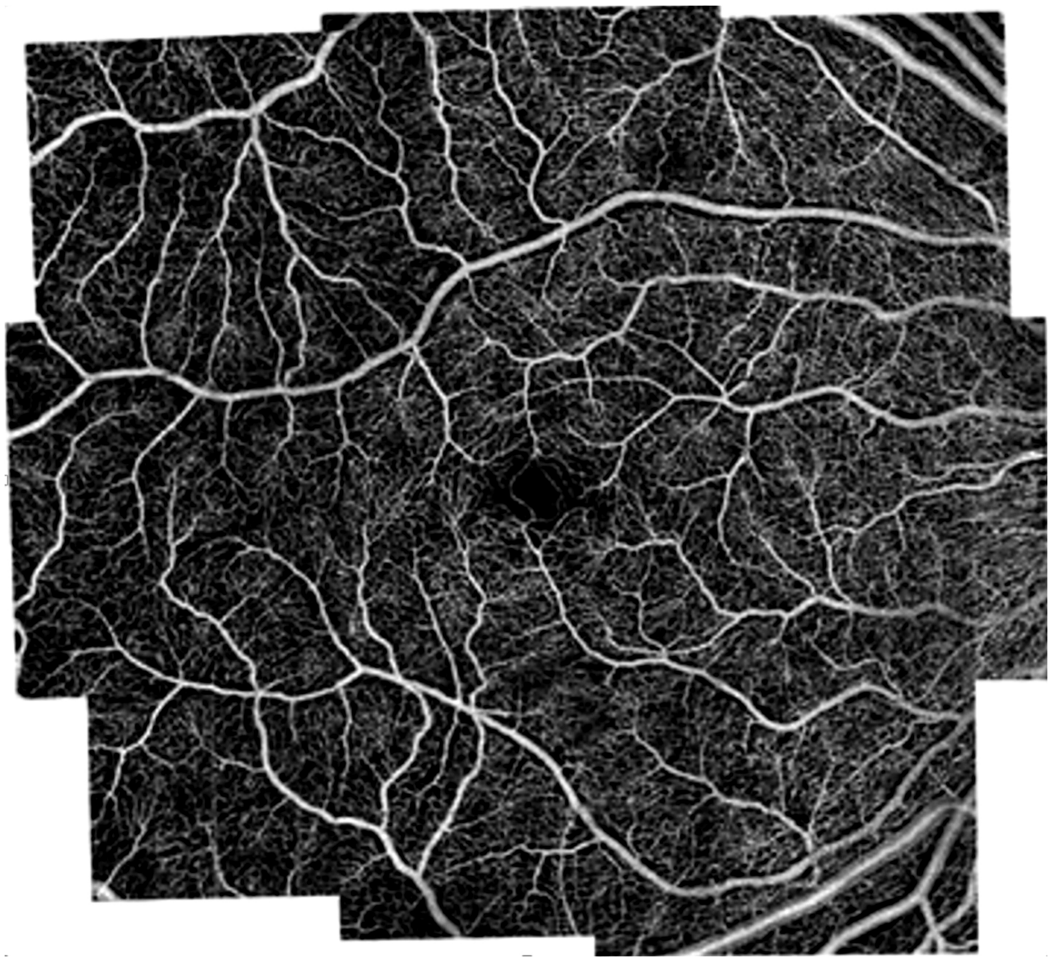

Fig. (1). OCT-A wide-field montage of vasculature in a normal retina. OCT-A images were acquired using the Angiovue software of the RTVue XR Avanti (Optovue, Inc., Fremont, CA) and montaged using Adobe Photoshop (San Jose, CA). Montage OCT-A imaging enables a large field of view like FFA with high-resolution of the retinal vasculature. Image unchanged from De Carlo, TE *et al.,Int J Retin Vitr* 1, 5 (2015) [4] and is used under the Creative Commons Attribution 4.0 International License (https://creativecommons.org/licenses/by/4.0/).

Fundoscopy and Fundus fluorescein angiography (FFA) are routinely used in the ophthalmology clinic as the standard of care to visualize retinal vasculature and vessel flow in retinal artery occlusion patients; however, the vascular networks

CHAPTER 10

Choroidal Neovascularization: Pathogenesis, Diagnosis, and Current Management Strategies

Sanjay Marasini[1] and **Miguel A. Quiroz-Reyes, MD**[2,*]

[1] *Department of Ophthalmology, The University of Auckland, Auckland, New Zealand*

[2] *Oftalmologia Integral ABC, Retina Department, Medical and Surgical Assistance Institution (Nonprofit Organization), Affiliated with the Postgraduate Studies Division, National Autonomous University of Mexico, Mexico City, Mexico*

Abstract: Choroidal neovascularization (CNV) is characterized by the growth of new blood vessels from the choroid to the subretinal pigment epithelium, subretinal space, or both. Newer diagnostic and treatment methods, such as, Optical Coherence Tomography Angiography and anti-vascular Endothelial Growth Factors, are becoming increasingly effective for CNV diagnosis and management, respectively. Anti-VEGF (Ranibizumab, Bevacizumab, and Aflibercept) treatment has become the first-line treatment for CNV and has replaced other methods, such as laser photocoagulation and photodynamic therapy. The current literature has established similar safety and efficacy of the three drugs (Ranibizumab, Bevacizumab, and Aflibercept) in the treatment of CNV, especially when the visual loss is mild. However, Aflibercept has been reported to result in slightly better long-term visual outcomes. Newer molecules such as Brolucizumab and Faricimab show the potential to decrease the treatment frequency and increase efficacy due to better penetration and by increasing drug concentration in the retina, addressing the limitations of the currently available drug options.

However, their investigation was in the early stages and may have taken some time before being seen in the clinic. Innovative methods for continuous drug delivery to the vitreous through the use of dedicated ocular implants filled with anti-VEGF drugs for controlled release (port delivery systems) have also shown promising results in clinical trials. The development of this technique is expected to reduce the total number of injections and maintain stable vision. Different clinical trial protocols across studies remain an issue in addressing research questions related to dosing frequency and gaps.

Keywords: Aflibercept, Anti-VEGF, Bevacizumab, Brolucizumab, Faricimab, Choroidal neovascularization (CNV), Myopic choroidal neovascularization, Age-related CNV, Idiopathic CNV, Inflammatory CNV.

* **Corresponding author Miguel A. Quiroz-Reyes, MD:** Oftalmologia Integral ABC, Retina Department, Medical and Surgical Assistance Institution (Nonprofit Organization), Affiliated with the Postgraduate Studies Division, National Autonomous University of Mexico, Mexico City, Mexico; Tel: +52 55 5217 2732; Fax: +52 55 1664 7180; E-mails: drquiroz@prodigy.net.mx and drquirozreyes7@gmail.com

Miguel A. Quiroz-Reyes and Virgilio Lima-Gomez (Eds.)

INTRODUCTION

Choroidal neovascularization (CNV) is characterized by the growth of new blood vessels from the choroid that extend into the subretinal pigment epithelium, subretinal space, or a combination of both (Fig. **1**). CNV is considered a nonspecific wound repair response to an underlying disease, the severity of which depends on the underlying condition [1]. The causes of CNV in people over 50 years of age are well characterized and include an array of retinal diseases, including age-related macular degeneration (AMD). However, this condition also occurs in young individuals. Cohen *et al.* (1996) [2] conducted a retrospective study to explore the relative incidence of various causes of CNV in people younger than 50 years of age (n = 363). They reported that CNV occurred mostly in myopic patients (62%), followed by pseudopresumed ocular histoplasmosis syndrome (12%), angioid streaks (5%), and various hereditary, traumatic, and inflammatory disorders (4%). The cause could not be identified in 17% of the cases. Visual prognosis of CNV is generally poor and may have a devastating effect on the quality of life of individuals. Yoshida *et al.* (2002) [3] studied the demographic and clinical data of patients with myopic CNV and followed them up for at least ten years after the onset of CNV. They explored the visual acuity readings during the ten years of the study period. They found that the long-term visual outcome of myopic CNV is extremely poor, dropping to 20/200 or less within 5–10 years after the onset of the disease. A good visual outcome is associated with younger age, smaller lesions, and earlier initiation of treatment.

TYPES OF CNV

Based on the proliferation pattern of new blood vessels in the retina, CNV is categorized as type 1 (subRPE), type 2 (subretinal), or type 3. In the Type 1 pattern, CNV grows between the RPE and Bruch's membrane. The vessels break through the Bruch's membrane and extend horizontally under the RPE in the natural cleavage between the basal laminar deposit and the Bruch's membrane, which has accumulated lipids (Fig. **2**). This growth pattern provides nutritional support to the RPE and outer retina [4]. Pfau *et al.* (2019) [5] evaluated the association between the presence of type 1 CNV and localized progression of atrophy in AMD. They found markedly reduced RPE atrophy progression in areas co-localized with quiescent and exudative type 1 CNV. The authors considered this to be a potential protective effect of type 1 CNV on the RPE and overlying neurosensory retina.

Fig. (1). CNV is characterized by the pathological growth of blood vessels involving the retinal pigment epithelium and Bruch's membrane and represents granulation tissue proliferation as seen in the wound-repair response. The growth of new vessels is known to be a final common pathway for several retinal conditions, such as AMD and idiopathic diseases.

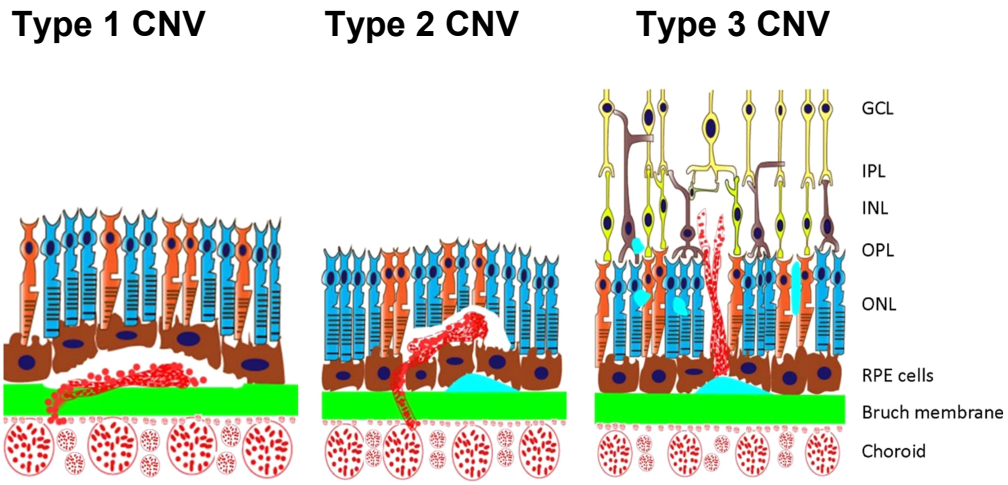

Fig. (2). Schematic diagram shows Type 1, Type 2, and Type 3 CNV. Type 1 CNV is characterized by an ingrowth of vessels originating from the choriocapillaris into the sub-RPE space; Type 2 CNV is the proliferation of new vessels arising from the choroid into the subretinal space; and Type 3 CNV is characterized by the downgrowth of vessels from the retinal vascular plexus toward the outer retina. Abbreviations: GCL, ganglion cell layer; IPL, inner plexiform layer; INL, inner nuclear layer; OPL, outer plexiform layer; ONL, outer nuclear layer; RPE, retinal pigment epithelium; MNV, macular neovascularization. The diagram was modified from the original publication by Qiang W *et al.* (2021) [7].

CHAPTER 11

Macular Perfusional Findings in Venous Obstructive Disease and Its Treatment: An OCT-A Evaluation

M. Naveed Yasin[1,2], Aftab Taiyab[2] and **Miguel A. Quiroz-Reyes, MD[3,*]**

[1] *Department of Ophthalmology, The University of Auckland, Auckland, New Zealand*

[2] *Department of Pathology and Molecular Medicine, McMaster University, Hamilton, Canada*

[3] *Oftalmologia Integral ABC, Retina Department, Medical and Surgical Assistance Institution (Nonprofit Organization), Affiliated with the Postgraduate Studies Division, National Autonomous University of Mexico, Mexico City, Mexico*

Abstract: The human retina is supplied by an extensive network of capillaries, where healthy blood flow to various parts of the retina, particularly the macula, is vital for visual functions. Any obstruction in blood flow, known as retinal vein occlusion (RVO), can reduce venous blood return. RVO can occur either at a central location (called central retinal vein occlusion [CRVO]) or a peripheral location (branch vein occlusion [BRVO]). Various techniques have been used to investigate blood flow to the retina and analyze different factors that may impact retinal blood flow. Optical coherence tomographic angiography (OCT-A) has emerged as one of the best methods, with several studies demonstrating its use to investigate changes in blood perfusion status, hemorrhage from blood vessels, and the presence of edema. Some studies have demonstrated that OCT-A is superior to other techniques.

Macular edema secondary to RVO is the most common complication that may affect visual acuity and lead to vision loss if left untreated. Several qualitative and quantitative changes caused by RVO can be detected using OCT-A, including vascular blood perfusion and vascular density. Several treatment options have been used to treat macular edema secondary to RVO and other complications. Laser photocoagulation therapy has been used extensively in the past with mixed outcomes. Glucocorticoids, especially dexamethasone (Ozurdex®), have also been used to treat macular edema secondary to RVO. Currently, anti-vascular endothelial growth factor (VEGF) agents are the gold standard for treating RVO. Ranibizumab and aflibercept are approved for the treatment of macular edema secondary to RVO, with faricimab expected to soon be approved.

* **Corresponding author Miguel A. Quiroz-Reyes, MD:** Oftalmologia Integral ABC, Retina Department, Medical and Surgical Assistance Institution (Nonprofit Organization), Affiliated with the Postgraduate Studies Division, National Autonomous University of Mexico, Mexico City, Mexico; Tel: +52 55 5217 2732; Fax: +52 55 1664 7180; E-mails: drquiroz@prodigy.net.mx and drquirozreyes7@gmail.com

Keywords: Macular perfusion, Venous retinal illness, Blood perfusion in retinal conditions, Choroidal neovascularization, Retinal vein occlusion, Macular ischemia, Macular edema, OCT-A.

INTRODUCTION

The current understanding of blood supply to the retina, specifically the macula, was developed by exploring and understanding the blood flow in primate eyes. Primate eyes are uniquely comparable to human eyes because of the presence of a high visual acuity area in the temporal region [1]. Several studies have revealed that blood is supplied by four layers of capillary plexuses to the retina: the superficial vascular plexus (SVP), intermediate capillary plexus (ICP), deep capillary plexus (DCP), and radial peripapillary capillary plexus (RPCP) [1 - 5]. For human eyes, these capillary plexuses have been confirmed by confocal microscopic examination ex vivo [6, 7]. Further examination of human eyes via optical coherence tomography angiography (OCT) has provided three-dimensional (3D) details of the blood-supplying vasculature of the retina, including the macular region [4].

Healthy blood flow to the retina, especially in the macular region, is essential for providing nutrients and oxygen to photoreceptors, neurons, and other cells that play important roles in vision. A decrease in blood flow to the retina, especially in the macular region, is a risk factor for neovascularization (NV) and/or macular edema [8]. Systemic cardiovascular conditions, such as atherosclerosis and hypertension, have been studied as risk factors for the development of NV [9, 10]. Previous studies have also explored the role of choroidal blood flow changes as a precursor to the development of age-related macular degeneration (AMD) [9]. A hemodynamic model of pathogenesis proposed by Friedman *et al.* showed that a decrease in macular blood flow could lead to atrophic AMD, whereas an increase in macular blood flow could lead to neovascular AMD [11]. This has been further investigated in studies where a decrease in foveal blood flow was observed in atrophic AMD when compared to healthy eyes [12]. Ischemia and hypoxia associated with atrophic AMD can trigger angiogenesis, which may explain the progression of atrophic AMD to neovascular AMD [13].

A decrease in retinal venous blood return is termed retinal vein occlusion (RVO) and can be triggered by atherosclerosis, inflammation, vasospasm, or compression [14, 15]. RVO can be central (CRVO) if obstruction occurs within or posterior to the optic nerve or branch (BRVO) if obstruction occurs within a branch; BRVO is more common than CRVO [16]. Another form of RVO, hemiretinal RVO (HRVO), can occur in a major fork. RVO can lead to macular edema and ischemia, triggering neovascularization and other complications [17]. It can also

cause optic neuropathy, vitreous hemorrhage, or retinal detachment [16]. Ischemic RVO is associated with poor visual acuity and requires treatment with anti-vascular endothelial growth factor (anti-VEGF) agents and corticosteroids [17, 18]. Diabetes, arterial hypertension, atherosclerosis, and thrombophilia are the common risk factors associated with RVO [16].

This chapter takes an aim explores the blood perfusion network in the retina, especially in the macular region. Retinal blood perfusion in healthy eyes was described along with optical coherence tomography angiography (OCT-A) images. After establishing the blood perfusion mechanism in healthy eyes, a detailed overview of the blood perfusion in RVO is presented with OCT-A images, presenting sequelae and macular perfusional repercussions. Treatment options for RVO and related complications are discussed in detail.

MACULAR BLOOD PERFUSION IN HEALTHY EYES

The retina is supplied by retinal and choroidal vessels, with the majority of blood supplied via the retinal artery, and almost all the blood is drained via the retinal vein [19]. The retinal and choroidal arteries form four major capillary plexuses (SVP, ICP, DCP, and RPCP) that supply optic nerves, photoreceptors, and surrounding cells. Campbell *et al.* investigated the blood supply to various regions of the retina using projection-resolved OCT-A (PR OCT-A) in healthy human eyes [4]. A significant improvement can be seen in Fig. (**1**) for studying detailed blood supply vasculature when compared to two-dimensional (2D) color fundus photographs. These findings are consistent with those of previous research carried out in primates and provide further details about the anatomy of the SVP, ICP, and DCP in the presence of an interconnecting layer (ICL) between these capillary plexuses.

Fig. (**2**) provides further exploration via OCT-A, with additional details about RPCP that seems to run along the dense nerve fiber layer (NFL), providing blood to the axons in the posterior pole around the optic nerve.

Supplementary Material

Table S1. Shapiro-Wilk normality test results in the Buckled group.

S. No.	Object	W	p value
1	Age	0.954	**0.001**
2	Preoperative BCVA (logMAR)	0.930	**0.001**
3	Postoperative BCVA (logMAR)	0.790	**0.001**
4	ERM Detection (weeks)	0.961	0.319
5	BCVA after ERM surgery (logMAR)	0.951	0.211
6	CSFT (microns)	0.888	**0.001**
7	Follow-up period (months)	0.959	**0.001**

The variables that do not follow a normal distribution are in bold writing ($p<0.05$).
W (Shapiro-Wilk normality test): BCVA: best corrected visual acuity; CSFT: central subfoveal thickness.

Table S2. Descriptive statistics for the numeric variables in the Buckle group.

S. No.	Object	Mean	Min	Max	Standard Deviation	Length of Sample (n=125)
1	Age (years)	44.34	18.00	76.00	15.94	125
2	Preoperative macula-off (weeks)	3.60	1.00	12.00	2.47	125
3	Preoperative BCVA (logMAR)	1.03	0.48	1.60	0.28	125
4	Postoperative BCVA (logMAR)	0.40	0.10	1.30	0.33	125
5	ERM detection (weeks)	11.93	5.00	22.00	4.59	125
6	BCVA after ERM surgery(logMAR)	0.43	0.18	0.70	0.14	125
7	CSFT (microns)	243.57	32.00	402.00	41.95	125
8	Follow-up period (months)	26.11	2.00	73.00	13.42	125

Non-parametric Mann-Whitney U-test. min: minimum; max: maximum; BCVA: best corrected visual acuity; ERM: epiretinal membrane; CSFT: central subfoveal thickness.

Table S3. Summarized statistics for the categorical variables in the Buckle group.

Variable	Value	n	Freq
Sex	Female	75	0.6
	Male	50	0.4

(Table S3) cont.....

Eye	Left	59	0.472
	Right	66	0.528
Preop Lens Status	Phakic	98	0.784
	Pseudophakic	27	0.216
Preop BCVA	20/100	26	0.208
	20/160	14	0.112
	20/200	35	0.28
	20/300	12	0.096
	20/400	21	0.168
	20/60	1	0.008
	20/70	3	0.024
	20/80	2	0.016
	20/800	11	0.088
Postop BCVA	20/100	11	0.088
	20/120	1	0.008
	20/160	1	0.008
	20/200	4	0.032
	20/25	16	0.128
	20/30	35	0.28
	20/300	3	0.024
	20/40	31	0.248
	20/400	6	0.048
	20/50	4	0.032
	20/60	8	0.064
	20/70	1	0.008
	20/80	4	0.032
Redetachment	No	114	0.912
	Yes	11	0.088

(Table S3) cont.....

Additional Surgery		114	0.912
	BUCKLE REVISION	4	0.032
	PHAKO-VITRECTOMY	3	0.024
	PHAKO-VITRECTOMY-ERM PEELING	1	0.008
	VITRECTOMY	2	0.016
	VITRECTOMY-ERM PEELING	1	0.008
Postop ERM proliferations	No	96	0.768
	Yes	29	0.232
ERM Surgery	No	98	0.784
	Yes	27	0.216
BCVA after ERM surgery		97	0.776
	20/100	2	0.016
	20/30	2	0.016
	20/40	7	0.056
	20/50	6	0.048
	20/60	4	0.032
	20/70	4	0.032
	20/80	3	0.024
Retinal perforation	No	118	0.944
	Yes	7	0.056
Submacular blood	No	120	0.96
	Yes	5	0.04
Through and through scleral drainage complication phenomenon	No	117	0.936
	Yes	8	0.064
Retinal entrapment	No	122	0.976
	Yes	3	0.024
Foveal contour OCT alterations	Normal	14	0.112
	Abnormal	19	0.152
	Normal	92	0.736
Ellipsoid band OCT alterations		14	0.112
	Disrupted	25	0.2
	Normal	86	0.688

(Table S3) cont.....

DONFL OCT defects		14	0.112
	Not Present	80	0.64
	Present	31	0.248
ELM line OCT alterations		15	0.12
	Abnormal	24	0.192
	Normal	86	0.688
mfERG registration		26	0.208
	Abnormal	54	0.432
	Normal	45	0.36
Microperimetry results		18	0.144
	Abnormal	51	0.408
	Normal	56	0.448

Fisher's exact test. freq: frequency; preop: preoperative: postop: postoperative: BCVA: best corrected visual acuity; CSFT: central subfoveal thickness; ERM: epiretinal membrane; DONFL: diffuse optic nerve fiber layer; ELM: external limiting membrane: mfERG: multifocal electroretinography.

Table S4. Correlations among the numeric variables in the Buckle group (sample size N=125 eyes).

	Age	Preoperative macula-off (weeks)	Preoperative BCVA (logMAR)	Postoperative BCVA (logMAR)	ERM Detection (weeks)	BCVA After ERM Surgery (logMAR)	CSFT (microns)	Follow-up Period (months)
Age	1 (p=NA)							
Preoperative macula-off (weeks)	0.12 (p=0.17)	1 (p=NA)						
Preoperative BCVA (logMAR)	0.01 (p=0.88)	0.04 (p=0.63)	1 (p=NA)					
Postoperative BCVA (logMAR)	-0.06 (p=0.48)	-0.02 (p=0.78)	0.02 (p=0.85)	1 (p=NA)				
ERM detection (weeks)	-0.27 (p=0.15)	-0.19 (p=0.31)	-0.19 (p=0.31)	0.06 (p=0.74)	1 (p=NA)			

(Table S4) cont.....

BCVA after ERM surgery (logMAR)	0.05 (p=0.79)	-0.21 (p=0.28)	0.26 (p=0.17)	**0.57 (p=0.00)**	0.04 (p=0.82)	1 (p=NA)		
CSFT (microns)	0.01 (p=0.9)	0.01 (p=0.93)	0.09 (p=0.37)	0.13 (p=0.17)	0.04 (p=0.85)	-0.06 (p=0.78)	1 (p=NA)	
Follow-up period (months)	-0.17 (p=0.06)	-0.17 (p=0.06)	0.03 (p=0.71)	**-0.2 (p=0.03)**	0.08 (p=0.68)	-0.05 (p=0.79)	0.12 (p=0.2)	1 (p=NA)

Spearman's rank correlation coefficient test. The significant correlations are in bold text. BCVA: best corrected visual acuity; ERM: epiretinal membrane; CSFT: central subfoveal thickness; NA: not applicable.

Table S5. Mann-Whitney U tests results in the Buckle group (N=125 eyes). (a) Preoperative best-corrected visual acuity (BCVA). (b) Postoperative BCVA. (c) BCVA after epiretinal membrane surgery.

(a) preoperative BCVA (logMAR) Mann-Whitney U tests results	-	-
Object	**U**	**p value**
Age	7875	**0.001**
Preoperative macula-off (weeks)	7140	**0.001**
Postoperative BCVA (logMAR)	201.5	**0.001**
ERM detection (weeks)	465	**0.001**
BCVA after ERM surgery (logMAR)	0	**0.001**
CSFT (microns)	6105	**0.001**
Follow-up period (months)	7875	**0.001**
(b) postoperative BCVA (logMAR) Mann-Whitney U tests results		
Object	**U**	**p value**
Age	7875	**0.001**
Preoperative macula-off (weeks)	7866	**0.001**
Preoperative BCVA (logMAR)	7301.5	**0.001**
ERM detection (weeks)	465	**0.001**
BCVA after ERM surgery (logMAR)	0	**0.001**
CSFT (microns)	6105	**0.001**
Follow-up period (months)	7875	**0.001**
(c) BCVA after ERM surgery (logMAR) Mann–Whitney U tests results		
Object	**U**	**p value**
Age	406	**0.001**

(Table S5) cont.....

Preoperative macula-off (weeks)	406	**0.001**
Preoperative BCVA (logMAR)	378	**0.001**
Postoperative BCVA (logMAR)	406	**0.001**
ERM detection (weeks)	406	**0.001**
CSFT (microns)	406	**0.001**
Follow-up period (months)	406	**0.001**

Mann-Whitney U tests. The statistically significant variables ($p < 0.05$) are in bold text. U test BCVA: best corrected visual acuity; ERM: epiretinal membrane; CSFT: central subfoveal thickness.

Table S6. Kruskal-Wallis test results in the Buckle group.

(a) Kruskal-Wallis test results of the preoperative best-corrected visual acuity (BCVA) with the categorical variables.

S. No.	Object	Kruskal-Wallis x^2.	df	p value	Number of eyes	No of NAs
1	Male	3.117	1	0.077	125	0
2	Eye	2.132	1	0.144	125	0
3	Preoperative Lens Status	0.130	1	0.718	125	0
4	**Preoperative BCVA**	**124.000**	**8**	**0.000**	**125**	**0**
5	Postoperative BCVA	5.342	12	0.946	125	0
6	Re-Detachment	1.018	1	0.313	125	0
7	Additional surgery	1.238	4	0.872	125	114
8	Postoperative ERM proliferations	0.035	1	0.851	125	0
9	ERM surgery	0.090	1	0.764	125	0
10	BCVA after ERM surgery	4.763	6	0.575	125	97
11	Retinal perforation	0.222	1	0.638	125	0
12	Submacular blood	1.057	1	0.304	125	0
13	Through and through	2.829	1	0.093	125	0
14	Retinal entrapment	0.001	1	0.980	125	0
15	Foveal contour	0.006	1	0.936	125	14
16	Ellipsoid	0.236	1	0.627	125	14
17	DONFL	1.581	1	0.209	125	14
18	ELM	0.384	1	0.535	125	15
19	mfERG	0.242	1	0.623	125	26
20	Microperimetry	0.653	1	0.419	125	18

(Table S6) cont.....

(b) Kruskal-Wallis test results of the postoperative BCVA with the categorical variables.

S. No.	Object	Kruskal-Wallis x^2.	df	p value	Number of eyes	No of NAs
1	Male	0.026	1	0.871	125	0
2	Eye	0.047	1	0.828	125	0
3	Preoperative Lens Status	0.234	1	0.629	125	0
4	Preoperative BCVA	3.950	8	0.862	125	0
5	**Postoperative BCVA**	**124.000**	**12**	**0.000**	**125**	**0**
6	**Re-Detachment**	**7.484**	**1**	**0.006**	**125**	**0**
7	Additional surgery	5.331	4	0.255	125	114
8	**Postoperative ERM proliferations**	**68.187**	**1**	**0.000**	**125**	**0**
9	**ERM surgery**	**63.098**	**1**	**0.000**	**125**	**0**
10	**BCVA after ERM surgery**	**13.048**	**6**	**0.042**	**125**	**97**
11	Retinal perforation	1.214	1	0.271	125	0
12	**Submacular blood**	**9.449**	**1**	**0.002**	**125**	**0**
13	Through and Through	0.357	1	0.550	125	0
14	Retinal Entrapment	0.612	1	0.434	125	0
15	**Foveal contour**	**15.821**	**1**	**0.000**	**125**	**14**
16	Ellipsoid	3.479	1	0.062	125	14
17	**DONFL**	**18.677**	**1**	**0.000**	**125**	**14**
18	ELM	0.303	1	0.582	125	15
19	**mfERG**	**20.558**	**1**	**0.000**	**125**	**26**
20	**Microperimetry**	**11.826**	**1**	**0.001**	**125**	**18**

(c) Kruskal-Wallis tests results of the BCVA after epiretinal membrane surgery with the categorical variables.

S. No.	Object	Kruskal-Wallis x^2.	df	p value	Number of eyes	No of NAs
1	Male	0.499	1	0.480	125	0
2	Eye	0.967	1	0.325	125	0
3	Preoperative Lens Status	1.070	1	0.301	125	0
4	Preoperative BCVA	6.587	7	0.473	125	0
5	Postoperative BCVA	11.572	6	0.072	125	0
6	Re-Detachment	0.428	1	0.513	125	0
7	Additional surgery	1.716	3	0.633	125	114

(Table S6) cont.....

8	Postoperative ERM proliferations	0.063	1	0.801	125	0
9	ERM surgery	0.063	1	0.801	125	0
10	BCVA after ERM surgery	27.000	6	**0.000**	125	97
11	Retinal perforation	1.847	1	0.174	125	0
12	Submacular blood	2.783	1	0.095	125	0
13	Through and Through	1.144	1	0.285	125	0
14	Retinal entrapment	0.776	1	0.378	125	0
15	Foveal contour	0.178	1	0.673	125	14
16	Ellipsoid	1.235	1	0.266	125	14
17	DONFL	1.230	1	0.267	125	14
18	ELM	0.138	1	0.710	125	15
19	mfERG	0.115	1	0.734	125	26
20	Microperimetry	1.033	1	0.310	125	18

The statistically significant variables ($p < 0.05$) are in bold text. df: difference no: number; NA: not applicable; BCVA: best corrected visual acuity; ERM: epiretinal membrane; DONFL: diffuse optic nerve fiber layer; ELM: external limiting membrane: mfERG: multifocal electroretinography.

Table S7. Generalized linear model results of the preoperative best-corrected visual acuity (BCVA), postoperative BCVA, and BCVA after epiretinal membrane surgery in the Buckle group (n=125 eyes).

Preoperative BVCA	**Estimate**	**Std. Error**	**t value**	**Pr(>|t|)**	
(Intercept)	0.972	0.033	29.046	**<2e-16**	***
Sex Male	0.106	0.051	2.07	**0.040**	*
Through and Through scleral drainage complication phenomenon	0.164	0.102	1.605	**0.111**	
Generalized	-	-	-	-	-
Postoperative BCVA	**Estimate**	**Std. Error**	**t value**	**Pr(>|t|)**	
(Intercept)	0.218	0.056	3.854	**0.001**	***
Postop ERM proliferations	0.676	0.035	19.055	**< 2e-16**	***
Retinal entrapment	-0.206	0.097	-2.112	**0.036**	*
Preop BCVA logMAR	0.029	0.052	0.567	0.572	
BCVA after ERM surgery	**Estimate**	**Std. Error**	**t value**	**Pr(>|t|)**	
(Intercept)	-0.170	0.130	-1.303	0.206	
Post BCVA logMAR	0.323	0.080	4.003	**0.001**	***

(Table S7) cont.....

Preop BCVA logMAR	0.194	0.072	2.694	**0.013**	*
Retinal perforation	0.151	0.067	2.251	**0.034**	*
Age	0.002	0.001	1.712	0.100	
Sex Male	-0.021	0.043	-0.498	0.623	

The statistically significant variables ($p < 0.05$) are in bold text and marked with *.
Pr: Probabilities using the t distribution, gives the p-value for that t-test; BCVA: best corrected visual acuity; Postop: postoperative; Preop: preoperative: ERM: epiretinal membrane.

Table S8. Shapiro-Wilk normality test results in the Vitrectomy group (n=105 eyes).

Object	**W**	**P value**
Age (years)	0.974	**0.039**
Macula-off (weeks)	0.924	**0.001**
Preoperative BCVA (logMAR)	0.923	**0.001**
Follow-up period (days)	0.971	**0.023**
BCVA before ERM-ILM removal (logMAR)	0.888	**0.001**
Final postoperative BCVA (logMAR)	0.924	**0.001**
CSFT (microns)	0.939	**0.008**
Follow-up period (months)	0.970	**0.023**

The variables that do not follow a normal distribution are in bold text ($p < 0.05$). BCVA: best corrected visual acuity; ERM: epiretinal membrane; ILM: internal limiting membrane; CSFT: central subfoveal thickness.

Table S9. Descriptive statistics for the numeric variables in the Vitrectomy group.

Object	**Mean**	**Min**	**Max**	**Standard Deviation**
Age (years)	47.92	18.00	76.00	14.60
Macula-off (weeks)	4.42	1.00	12.00	2.56
Preoperative BCVA (logMAR)	1.06	0.54	1.60	0.27
Follow-up period (months)	24.2	1.0	58.66	13.02
BCVA before ERM-ILM removal (logMAR)	0.52	0.10	1.30	0.36
ERM detection (weeks)	13.75	5.00	30.00	5.33
Final postoperative BCVA (logMAR)	0.37	0.10	1.00	0.20
CSFT (microns)	256.55	198.00	320.00	35.16
Follow-up period (months)	23.42	1.00	57.00	12.98

Wilcoxon rank sum test. Min: minimum; Max: maximum; BCVA: best corrected visual

acuity; ERM: epiretinal membrane; ILM: internal limiting membrane; CSFT: central subfoveal thickness.

Table S10. Summarized statistics for the categorical variables in the vitrectomy group (peeling and nonpeeling groups).

Variable	Group	n	freq	% freq
Additional Surgery	BUCKLE REVISION	3	0.03	2.9%
	No	92	0.88	87.6%
	PHAKO VITRECTOMY ERM PEELING	1	0.01	1.0%
	VITRECTOMY	2	0.02	1.9%
	VITRECTOMY REVISION	7	0.07	6.7%
DONFL	Absent	34	0.32	32.4%
	Present	60	0.57	57.1%
	NA	11	0.10	10.5%
Ellipsoid	Disrupted	29	0.28	27.6%
	Normal	76	0.72	72.4%
ELM	Disrupted	27	0.26	25.7%
	Normal	74	0.70	70.5%
	NA	4	0.04	3.8%
ERM 2nd Surgery	VIT and MACULA REVISION	1	0.01	1.0%
	VIT REVISION ERM-ILM REMOVAL	45	0.43	42.9%
	VIT REVISION ERM-ILM REMOVAL	5	0.05	4.8%
	VIT REVISION ERM-ILM REMOVAL	1	0.01	1.0%
	NA	53	0.50	50.5%
Eye	Left	50	0.48	47.6%
	Right	55	0.52	52.4%
First Surgery	BUCKLE	27	0.26	25.7%
	ONLY VITRECTOMY	68	0.65	64.8%
	VIT ERM-ILM REMOVAL	10	0.10	9.5%
Foveal contour	Abnormal	24	0.23	22.9%
	Normal	77	0.73	73.3%
	NA	4	0.04	3.8%
Sex	Female	37	0.35	35.2%
	Male	68	0.65	64.8%

(Table S10) cont.....

mfERG	Abnormal	43	0.41	41.0%
	Normal	30	0.29	28.6%
	NA	32	0.30	30.5%
Microperimetry	Abnormal	35	0.33	33.3%
	Normal	42	0.40	40.0%
	NA	28	0.27	26.7%
Postoperative ERM proliferations	No	54	0.51	51.4%
	Yes	51	0.49	48.6%
Preoperative ERM proliferations	No	55	0.52	52.4%
	Yes	50	0.48	47.6%
Preop Lens Status	Phakic	68	0.65	64.8%
	Pseudophakic	37	0.35	35.2%
Recurrent RRD	No	92	0.88	87.6%
	Yes	13	0.12	12.4%

Fisher's exact test. freq: frequency; ERM: epiretinal membrane; DONFL: diffuse optic nerve fiber layer; ELM: external limiting membrane; VIT: vitrectomy; ILM: internal limiting membrane; mfERG: multifocal electroretinography; RRD: rhegmatogenous retinal detachment.

Table S11. Descriptive statistics with respect to the Vitrectomy (preoperative ERM proliferations) group (nonpeeling and peeling).

Vitrectomy groups	**Nonpeeling**	**Peeling**	**p**	-
	(N=55)	(N=50)	-	-
	-	-	-	-
Age	50.455 ± 13.52	45.140 ±15.36	0.054	-
	-	-	-	-
Sex	-	-	1	-
- Female	19 (34.545%)	18 (36.0%)	-	-
- Male	36 (65.455%)	32 (64.0%)	-	-
	-	-	-	-
Eye	-	-	0.698	-
- Left	25 (45.455%)	25 (50.0%)	-	-
- Right	30 (54.545%)	25 (50.0%)	-	-
	-	-	-	-

(Table S11) cont.....

Preoperative Lens Status	-	-	0.068	-
- Phakic	31 (56.364%)	37 (74.0%)	-	-
- Pseudophakic	24 (43.636%)	13 (26.0%)	-	-
	-	-	-	-
Macula-off (weeks)	4.527 ±2.403	4.300 ±2.750	0.425	-
	-	-	-	-
Preoperative BCVA (logMAR)	1.036 ±0.258	1.077 ±0.277	0.386	-
	-	-	-	-
Follow-up period (days)	768.6 ±373.01	679.90 ±407.98	0.131	-
	-	-	-	-
First Surgery	-	-	**0**	***
- BUCKLE	0 (0.0%)	27 (54.0%)	-	-
- ONLY VITRECTOMY	55 (100.000%)	13 (26.0%)	-	-
- VIT ERM and ILM REMOVAL	0 (0.0%)	10 (20.0%)	-	-
BCVA Before ERM-ILM removal (logMAR)	**0.297 ±0.23**	**0.756 ±0.319**	**0.001**	***
Recurrent RRD			**0.001**	***
- No	54 (98.182%)	38 (76.0%)		
- YES	1 (1.818%)	12 (24.0%)		
Additional Surgery			**0.004**	***
- BUCKLE REVISION	0 (0.0%)	3 (6.0%)		
- No	54 (98.182%)	38 (76.0%)		
- PHAKO VITRECTOMY ERM PEELING	0 (0.0%)	1 (2.0%)		
- VITRECTOMY	0 (0.0%)	2 (4.0%)		
- VITRECTOMY REVISION	1 (1.818%)	6 (12.0%)		
ERM Detection (weeks)	**18.00 ±6.45**	**12.575 ±4.385**	**0.009**	***
ERM 2nd Surgery			**0**	***
- VIT and MACULA REVISION	0 (0.0%)	1 (2.439%)		
- VIT REVISION ERM and ILM	5 (45.455%)	40 (97.561%)		
- VIT REVISION ERM and ILM REMOVAL	5 (45.455%)	0 (0.0%)		
- VIT REVISION ERM.ILM REMOVAL	1 (9.091%)	0 (0.0%)		
Final Postoperative BCVA (logMAR)	**0.280 ±0.192**	**0.477 ±0.161**	**0.001**	***

(Table S11) cont.....

CSFT (microns)	266.71 ±32.75	253.073 ±35.66	0.173	
Foveal Contour			**0.002**	***
- Abnormal	6 (11.321%)	18 (37.5%)		
- Normal	47 (88.679%)	30 (62.5%)		
Ellipsoid integrity			0.828	
- Disrupted	16 (29.091%)	13 (26.0%)		
- Normal	39 (70.909%)	37 (74.0%)		
DONFL defects			**0**	***
- Absent	39 (88.63%)	21 (42.0%)		
- Present	5 (11.36%)	29 (58.0%)		
ELM line appearance			0.654	
- Disrupted	16 (29.091%)	11 (23.913%)		
- Normal	39 (70.909%)	35 (76.087%)		
mfERG result			**0**	***
- Abnormal	13 (33.333%)	30 (88.235%)		
- Normal	26 (66.667%)	4 (11.765%)		
Microperimetry evaluation			**0**	***
- Abnormal	11 (25.581%)	24 (70.588%)		
- Normal	32 (74.419%)	10 (29.412%)		
Follow-up period (months)	24.80 ±12.34	21.880 ±13.324	0.133	

The p-values (p) are the results from the Wilcoxon rank sum test for the numerical variables and Fisher's Exact test for the categorical variables. The variables that showed a statistically significant difference ($p < 0.05$) among the groups of the peeling (preoperative ERM proliferation) are in bold text and marked with *. sig: significance ; BCVA: best corrected visual acuity; VIT: vitrectomy; ERM: epiretinal membrane; ILM: internal limiting membrane; RRD: rhegmatogenous retinal detachment; CSFT: central subfoveal thickness; DONFL: diffuse optic nerve fiber layer; ELM: external limiting membrane: mfERG: multifocal electroretinography.

Table S12. Correlations among the numeric variables in the Vitrectomy group (peeling and nonpeeling groups).

	Age	**Preoperative Macula-Off (weeks)**	**Preoperative BCVA (logMAR)**	**BCVA Before ERM and ILM removal (logMAR)**	**ERM Detection (Weeks)**	**Final Postoperative BCVA (logMAR)**	**CSFT (microns)**	**Follow-up period (months)**
Age	1							
Preoperative Macula-off (weeks)	0.03 (p=0.78)	1						
Preoperative BCVA (logMAR)	-0.07 (p=0.47)	0.04 (p=0.68)	1					
BCVA Before ERM and ILM removal (logMAR)	-0.18 (p=0.07)	-0.16 (p=0.1)	-0.10 (p=0.33)	1				
ERM Detection (weeks)	-0.18 (p=0.21)	0.03 (p=0.83)	**-0.29 (p=0.04)**	-0.16 (p=0.26)	1			
Final Postoperative BCVA (logMAR)	-0.04 (p=0.72)	-0.05 (p=0.62)	0.10 (p=0.3)	**0.78 (p=0)**	0.04 (p=0.76)	1		
CSFT (microns)	0.15 (p=0.28)	**0.32 (p=0.02)**	0.02 (p=0.89)	-0.14 (p=0.32)	0.02 (p=0.89)	0.02 (p=0.88)	1	
Follow-up period (months)	-0.14 (p=0.18)	-0.08 (p=0.42)	0.09 (p=0.36)	-0.2 (p=0.05)	0.12 (p=0.42)	-0.05 (p=0.61)	-0.08 (p=0.6)	1

Wilcoxon rank sum test. The p-values in parenthesis (p); significant correlations ($p < 0.05$) are in bold text. BCVA: best corrected visual acuity; ERM: epiretinal membrane; ILM: internal limiting membrane; CSFT: central subfoveal thickness. Spearman Rank Test nonpeeling sample=55 eyes. Peeling sample=50 eyes.

Table S13. Mann-Whitney U tests results in the Vitrectomy group (peeling and nonpeeling groups). (a) Preoperative best-corrected visual acuity (BCVA). (b) Postoperative BCVA. (c) Final BCVA.

(a) preoperative BCVA (logMAR) Mann-Whitney U tests results		
Object	**U**	**p-value**
Age	5565	**0.001**
Macula-off (weeks)	5341	**0.001**

(Table S13) cont.....

Follow-up period (days)	5565	**0.001**
BCVA before ERM-ILM removal (logMAR)	238	**0.001**
ERM detection (weeks)	1326	**0.001**
Final postoperative BCVA (logMAR)	0	**0.001**
CSFT (microns)	1540	**0.001**
Follow-up period (months)	4950	**0.001**
(b) postoperative BCVA (logMAR) Mann-Whitney U tests results		
Object	**U**	**p-value**
Age	5565	**0.001**
Macula-off (weeks)	5556	**0.001**
Preoperative BCVA (logMAR)	4712	**0.001**
Follow-up period (days)	5565	**0.001**
ERM detection (weeks)	1326	**0.001**
Final postoperative BCVA (logMAR)	101.5	**0.001**
CSFT (microns)	1540	**0.001**
Follow-up period (months)	5049	**0.001**
(c) final BCVA after ERM proliferation removal (logMAR)		
Object	**U**	**p-value**
Age	5565	**0.001**
Macula-off (weeks)	5565	**0.001**
Preoperative BCVA (logMAR)	5460	**0.001**
Follow-up period (days)	5565	**0.001**
BCVA before ERM-ILM removal (logMAR)	1074.5	**0.001**
ERM detection (weeks)	1326	**0.001**
CSFT (microns)	1540	**0.001**
Follow-up period (months)	5050	**0.001**

The statistically significant variables ($p < 0.05$) are in bold text. BCVA: best corrected visual acuity; ERM: epiretinal membrane; ILM: internal limiting membrane; CSFT: central subfoveal thickness.

Table S14. Kruskal-Wallis test results in the Vitrectomy group (peeling and nonpeeling groups). (a) Preoperative best-corrected visual acuity (BCVA). (b) Postoperative BCVA. (c) Final BCVA.

(a) preoperative BCVA (logMAR) Kruskal-Wallis tests results			
Object	**Kruskal-Wallis x^2.**	**df**	**p-value**
Male	0.458	1	0.499
Eye	1.878	1	0.171
Preoperative Lens Status	1.640	1	0.200
Preoperative ERM proliferations	0.760	1	0.383
First Surgery	1.055	2	0.590
BCVA Before ERM-ILM removal	9.412	12	0.667
Recurrent RRD	0.208	1	0.649
Additional surgery	1.360	4	0.851
Postoperative ERMs	0.038	1	0.846
ERM 2nd surgery	3.135	3	0.371
Final Postoperative BCVA	11.718	10	0.304
Foveal contour abnormalities	0.385	1	0.535
Ellipsoid disruption	4.175	1	**0.041**
DONFL defects	1.402	1	0.236
ELM line alterations	0.144	1	0.704
mfERG alterations	0.109	1	0.741
Microperimetry alterations	1.623	1	0.203
(b) postoperative BCVA (logMAR) Kruskal-Wallis tests results			
Object	**Kruskal-Wallis x^2.**	**df**	**p-value**
Male	0.355	1	0.552
Eye	0.001	1	0.979
Preoperative Lens Status	6.083	1	**0.014**
Preoperative BCVA	12.845	8	0.117
Preoperative ERM proliferations	50.177	1	**0.001**
First surgery	47.013	2	**0.000**
Recurrent RRD	11.364	1	**0.001**
Additional surgery	12.324	4	**0.015**
Postoperative ERM proliferations	68.366	1	**0.001**

(Table S14) cont.....

ERM 2nd surgery	5.469	3	0.141
Foveal Contour abnormalities	10.021	1	**0.002**
Ellipsoid disruption	1.091	1	0.296
DONFL defect	19.206	1	**0.001**
ELM line alterations	0.746	1	0.388
mfERG alterations	31.253	1	**0.001**
Microperimetry alterations	19.749	1	**0.001**
(c) final BCVA after ERM proliferation removal (logMAR)			
Object	**Kruskal-Wallis x^2.**	**df**	**p-value**
Male	1.561	1	0.211
Eye	0.121	1	0.728
Preoperative Lens Status	1.855	1	0.173
Preoperative ERM proliferations	33.337	1	**0.001**
First surgery	13.877	2	**0.001**
Recurrent RRD	9.223	1	**0.002**
Additional surgery	10.697	4	**0.030**
Postoperative ERM proliferations	38.068	1	**0.001**
ERM 2nd surgery	1.113	3	0.774
Foveal contour abnormalities	6.168	1	**0.013**
Ellipsoid disruption	0.894	1	0.344
DONFL defect	16.777	1	**0.001**
ELM line alterations	0.375	1	0.540
mfERG alterations	16.522	1	**0.001**
Microperimetry alterations	13.150	1	**0.001**

The statistically significant variables ($p < 0.05$) are in bold text. df: degrees of freedom: BCVA: best corrected visual acuity; ERM: epiretinal membrane; ILM: internal limiting membrane; RRD: rhegmatogenous retinal detachment; DONFL: diffuse optic nerve fiber layer; ELM: external limiting membrane: mfERG: multifocal electroretinography.

Table S15. Generalized linear model results in the Vitrectomy group (peeling and nonpeeling groups). (a) Preoperative best-corrected visual acuity (BCVA). (b) Postoperative BCVA. (c) Final BCVA.

(a) preoperative BCVA (logMAR) GLM results				
	Estimate	**SE**	**t value**	**p**
(Intercept)	1.055	0.026	40.60	**0.001**
(b) postoperative BCVA (logMAR) GLM results				
	Estimate	**SE**	**t value**	**p**
(Intercept)	0.515	0.067	7.72	**0.001**
Postoperative ERM proliferations	0.448	0.050	8.97	**0.001**
First surgery - ONLY VITRECTOMY	-0.235	0.055	-4.30	**0.001**
First surgery - VIT ERM and ILM REMOVAL	0.034	0.090	0.38	0.704
Macula-off (weeks)	-0.019	0.008	-2.50	**0.014**
Recurrent RRD	0.118	0.061	1.94	0.055
(c) final BCVA after ERM proliferation removal (logMAR) GLM results				
	Estimate	**SE**	**t value**	**p**
(Intercept)	-0.213	0.070	-3.05	**0.003**
BCVA Before ERM-ILM removal (logMAR)	0.552	0.046	11.98	**0.001**
First Surgery - ONLY VITRECTOMY	0.201	0.038	5.22	**0.001**
First Surgery - VIT ERM and ILM REMOVAL	0.275	0.051	5.42	**0.001**
Preoperative BCVA (logMAR)	0.106	0.046	2.29	**0.024**
Gender - Male	0.052	0.026	2.03	**0.045**

The statistically significant variables ($p < 0.05$) are in bold text. BCVA: best corrected visual acuity; GLM: generalized linear models; SE: standard error; ERM: epiretinal membrane; VIT: vitrectomy; ILM: internal limiting membrane; mfERG: multifocal electroretinography; RRD: rhegmatogenous retinal detachment.

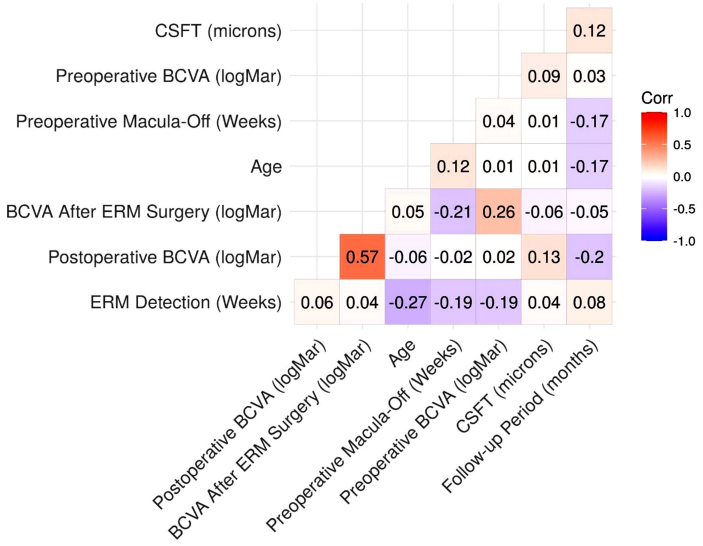

Additional Fig. S1. The Spearman's rank correlation coefficient test showed that there was a moderate to strong positive correlation (rho= 0.57, p<0.01) of the postoperative BCVA in logMAR units with the BCVA after ERM surgery. In addition, there was a weak negative correlation (rho = -0.2, p<0.05) between postoperative BCVA in logMAR units and follow-up period in months.

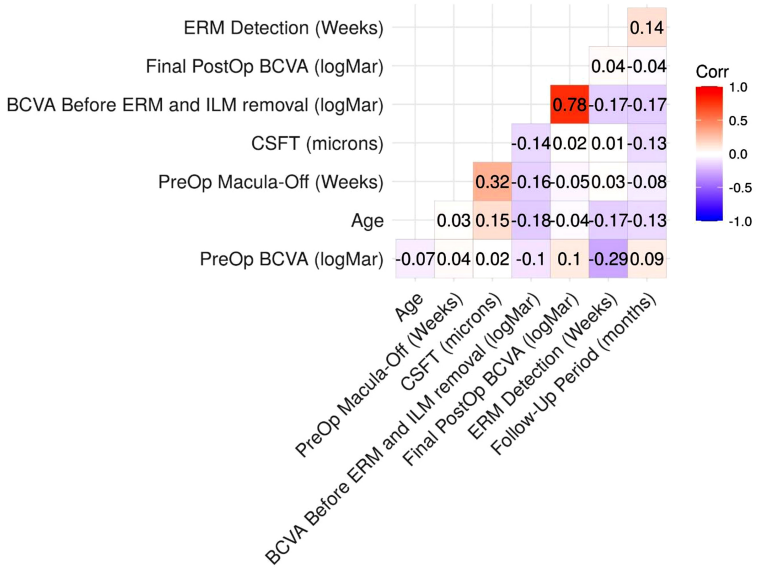

Additional Fig. S2. The Spearman's rank correlation coefficient test showed a weak positive correlation (rho= 0.32, p<0.05) between the preoperative period with the macula-off in weeks and the CSFT findings in microns; it also showed a weak negative correlation (rho= -0.29, p<0.05) between the preoperative BCVA in logMAR units and ERM detection in weeks.

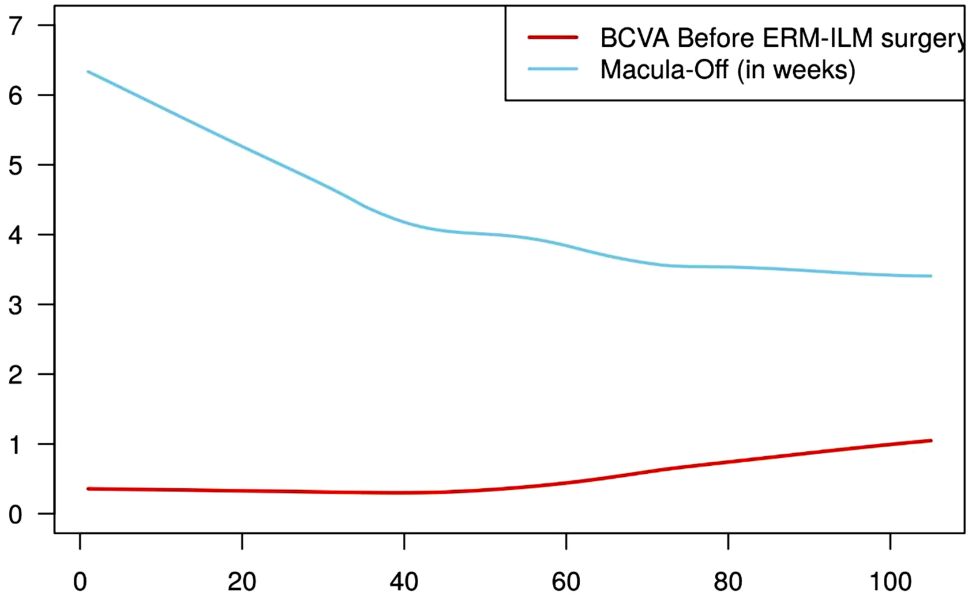

Additional Fig. S3. Postoperative BCVA was significantly negatively associated when only vitrectomy (nonpeeling group) was performed in the first surgery variable (coefficient = -0.23, $p<0.01$) and significantly negatively associated with the variable preoperative period of macula-off in weeks (coefficient= -0.02, $p<0.05$).

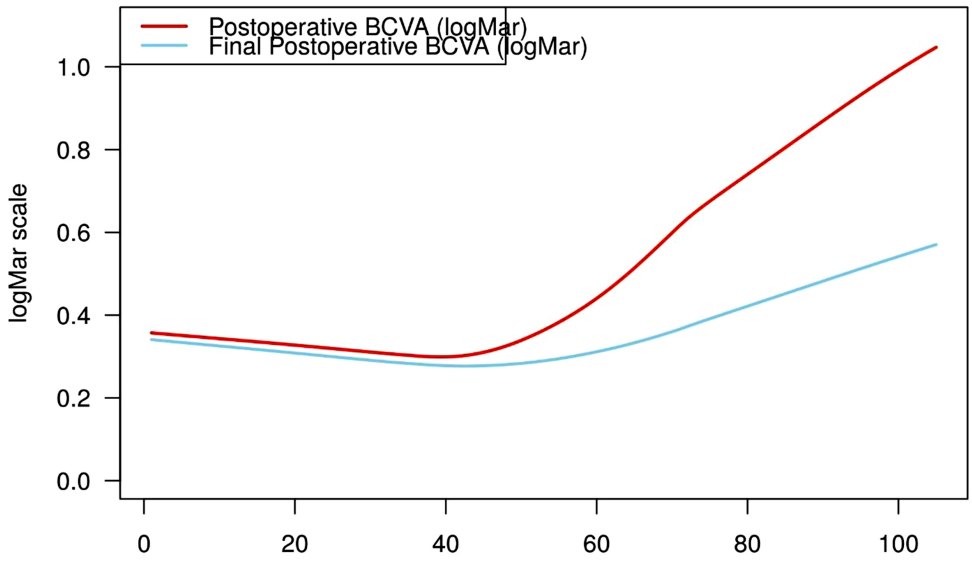

Additional Fig. S4. The GLM for the final BCVA in log MAR units after ERM proliferation removal showed that it was significantly positively associated ($p>0.01$) with the postoperative.

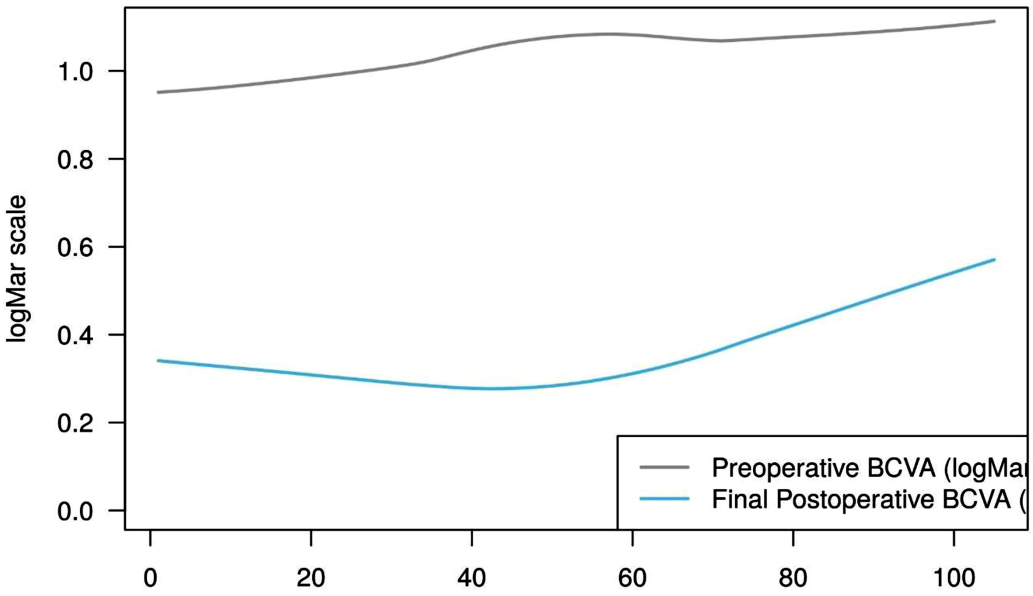

Additional Fig. S5. Shows when only vitrectomy was the first surgery variable, and with the preoperative BCVA.

SUBJECT INDEX

A

B

C

D

E

F

G

H

I

L

M

N

O

P

R

S

T

V

Y

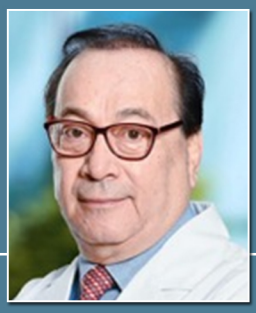

Miguel A. Quiroz-Reyes

Prof. Miguel A. Quiroz-Reyes is an ophthalmologist, retina specialist, and macula surgeon. He is a former president of the Mexican Retina Association and member of the Mexican Society of Ophthalmology, American Academy of Ophthalmology, American Society of Retina Specialists and PAAO. He is certified in ophthalmology and earned his master's degree from the Faculty of Medicine and Mexican Board of Ophthalmology affiliated with The National Autonomous University of Mexico. His goals include teaching, scientific writing, developing state-of-the art surgery techniques and assisting academical activities. His passion for the retina can be traced back to 1989 in Boston, where he specialized from Schepens Eye Research, which is affiliated with Harvard Medical School.

Virgilio Lima-Gomez

Prof. Virgilio Lima-Gomez is an ophthalmologist, retina specialist and a DSc Research in Medicine. He is an attending physician and surgeon, former head of the Ophthalmology Service, and of the Research Division at Hospital Juárez de México. He is a member of the Mexican Ophthalmology Society, Mexican Retina Association, Mexican Academy of Surgery and National Academy of Medicine of Mexico. He is an ophthalmology professor at Universidad Nacional Autonoma de Mexico, member of the National Researchers System. He was awarded the National Research Prize by Fundacion Mexicana para la Salud in 2008. His current research focuses on optical coherence tomography angiography, diabetic retinopathy and myopia.